NASA-CR-199390

Final Report

Submitted to:	NASA Langley Research Center
Grant Title:	ROBUST STABILITY OF SECOND-ORDER SYSTEMS
Grant Number:	NAG-1-1397
Organization:	Georgia Institute of Technology Atlanta, GA 30332-0150
Principal Investigator/ Project Director:	Dr. C.-H. Chuang Professor of School of Aerospace Engineering Georgia Institute of Technology Atlanta, GA 30332-0150 Phone: 404-894-3075 Fax: 404-894-2760 e-mail: ch.chuang@aerospace.gatech.edu
Period Covered:	February 24, 1992 to June 30, 1995
Date of Submission:	September 29, 1995

(NASA-CR-199390) ROBUST STABILITY OF SECOND-ORDER SYSTEMS Final Report, 24 Feb. 1992 - 30 Jun. 1995 (Georgia Inst. of Tech.) 39 p

N96-13349

Unclas

G3/63 0067503

Project Conclusions

Research results of this grant (NAG-1-1397) entitled ROBUST STABILITY OF SECOND-ORDER SYSTEMS sponsored by NASA Langley Research Center are included in the following four papers:

1. "Controller Designs for Positive Real Second-Order Systems," Proceedings of 1st International Conf. on Motion and Vibration Control, Yokohama, September 1992.
2. "A Robust Controller for Second-Order Systems using Acceleration Measurements," Proceedings of AIAA Guidance, Navigation and Control Conference, Monterey, August 1993.
3. "A Passivity Based Controller for Free Base Manipulator," Proceedings of AIAA Guidance, Navigation and Control Conference, Monterey, August 1993.
4. "Nonlinear Control of Space Manipulators with Model Uncertainty," Proceedings of AIAA Guidance, Navigation and Control Conference, Scottsdale, August 1994.

The four papers have been published in the conference proceedings as indicated above and they are either in the review process or to be submitted for technical journal publication. The objectives of this project have been demonstrated in the four papers.

In the paper "Controller Designs for Positive Real Second-Order Systems," necessary and sufficient conditions for positive realness of second-order SISO systems have been derived. For the MIMO case, two designs using different choices of output variables have been presented for the system without velocity output. And a possible control method for such systems has been examined, illustrated by the simple example.

The paper "A Robust Controller for Second-Order Systems using Acceleration Measurements" presented an interesting practical control method. Only acceleration at certain locations of the system needs to be measured by using common available accelerometers. The design is model independent and no knowledge of the constants of the dynamic system is required. Any strictly positive real controller can be used. Thus it is possible to choose one that yields a satisfactory transient response.

In the paper "A Passivity Based Controller for Free Base Manipulator," a control method based on feedback linearization and passivity concepts that was proposed earlier for fixed base robots is modified and extended to the case of space robots. The control law

results in asymptotic joint angle tracking in the face of bounded uncertainties. For the first time, closed-loop simulation results are presented using this control method. For the one link and two link manipulator examples illustrated in the paper, the control method shows promising results. Specifically, it was shown that significant simplifications to the nominally complex feedback linearization controller are possible when the proposed robust control method is used for synthesis.

In the paper "Nonlinear Control of Space Manipulators with Model Uncertainty," a nonlinear dynamic model was obtained for space manipulators with uncontrolled base. A robust control method based on feedback linearization and passivity concepts was proposed for space manipulators. The method is applicable to fixed base manipulators as well. The control law results in asymptotic joint angle tracking in the face of bounded uncertainties such as those due to imprecise friction modeling.

Further research is needed to extend the robust stability results of this study to a commercial application. Structure damage is a crucial problem of public safety. The robust stability feature ensures that an installation of active controllers will always improve the safety and performance. If the controllers of this study are validated by experiments, transfer of this robust stability technology to commercial sectors will be accelerated.

Paper presented at the 1st International Conf. on Motion and Vibration Control, Yokohama, September 1992
Session : Control of Aerospace Structure II

CONTROLLER DESIGNS FOR POSITIVE REAL SECOND-ORDER SYSTEMS

C.-H. Chuang, Olivier Courouge, and J. N. Juang
Georgia Institute of Technology, Atlanta, GA 30332, U.S.A.

ABSTRACT

It has been shown recently in [1, 2] how virtual passive controllers can be designed for second-order dynamic systems to achieve robust stability. The virtual controllers were visualized as systems made up of spring, mass and damping elements. In this paper, a new approach emphasizing on the notion of positive realness to the same second-order dynamic systems is used. Necessary and sufficient conditions for positive realness are presented for scalar spring-mass-dashpot systems. For multi-input multi-output systems, we show how a mass-spring-dashpot system can be made positive real by properly choosing its output variables. In particular, sufficient conditions are shown for the system without output velocity. Furthermore, if velocity cannot be measured then the system parameters must be precise to keep the system positive real. In practice, system parameters are not always constant and cannot be measured precisely. Therefore, in order to be useful positive real systems must be robust to some degrees. This can be achieved with the design presented in this paper.

KEY WORDS: positive real, second-order system, multivariable system, controller design

1. INTRODUCTION

The concept of positive realness was first used in network theory. A function that can realized as the driving point impedance of a passive network is called positive real (PR). In general, a linear system is called positive real (PR) when it is possible to define an energy term that is not generated within the system. PR systems have many important applications in control theory; however, much attention has been paid in the literature for finding criteria for positive realness of linear systems (see [3]). PR systems have also been used for shape control of large flexible structures. Nevertheless, positive realness of multivariable second-order systems was never studied in details. For most PR designs in the literature, the output of the plant is usually a vector of velocity sensors collocated with a set of points actuators.

In this paper, we use a more general approach for PR systems and present several possible PR designs. First we review basic definitions and theorems and clarify the physical meaning of positive realness. Then we find necessary and sufficient conditions for positive realness of single-input single-output spring-mass-dashpot systems. For multi-input multi-output systems, the Kalman-Yakubovitch Lemma is used to find sufficient conditions. The sufficient conditions state that given a spring-mass-dashpot system it is possible to define an output variable which will make the system PR. Since certain variables of the system may not be always measurable, we consider the positive realness under restrictions of available measurements. With uncertainty in the system parameters the positive realness of a system without velocity output will not hold anymore. In this case we present a design method using a feed-forward loop to achieve positive realness. The robustness of a general positive real second-order system can thus be achieved by using this method. Finally, the design method is demonstrated in a simple example.

2. REVIEW OF DEFINITIONS AND THEOREMS

2.1 Positive Real Systems

Definition 1 [5]: An n×n matrix is called positive real if it satisfies all the following conditions:

1. G(s) is real rational.
2. G(s) is analytic in Re(s)>0.
3. Poles of G(s) on the imaginary axis are simple and the residues of these poles are Hermitian and positive semi-definite.
4. $G(j\omega)+G^*(j\omega) \geq 0$ for all real ω.

The above definition does not have any physical interpretation. Another definition of PR systems is given in the time domain, which uses the concept of passivity and allows a physical interpretation of positive realness. This definition is shown in the following.

Definition 2 [5]: Let a linear time-invariant system have the a minimum state space representation (A,B,C,D). Let u be an m×1 control vector, y be an m×1 observation vector, and x be an n×1 state vector. Then the system is passive if and only if there exist two functions $\xi(x)$ and $\lambda(x,u)$ such that the scalar product of input with output can be expressed for all $t \geq t_0$ by

$$\int_{t_0}^{t} y^T u \, dt = [\xi(x)]_{t_0}^{t} + \int_{t_0}^{t} \lambda(x,u)\, dt \qquad (1)$$

with $\lambda(x,u) \geq 0$ for all x and u.

Remark 1: $y^T u$ is the external power input and $-\lambda(x,u)$ is the internal power generation. Equation (2) indicates that the variation of stored energy is equal to the external energy input plus the internal energy generation. Since $\lambda(x,u) \geq 0$, the internal power generation is always negative and so is the internal energy generation at any time t. As a consequence, passive systems are systems that do not generate energy. Nevertheless, the energy will not always have a physical interpretation. In the above definition $\xi(x)$ can be any function of x, and it may not have any obvious physical meaning.

The following theorem states a relationship between linear PR systems and passive systems.

Theorem 1 [5]: Consider a time-invariant linear system with transfer matrix G(s). G(s) is positive real if and only if the system is passive.

Hence positive real linear systems are linear systems for which the energy is not internally generated by the system. Positive real matrices can also be characterized in the time domain by using the following Kalman-Yakubovich Lemma.

Theorem 2. Kalman-Yakubovich (K-Y) Lemma [5]: Let G(s) be an n×n real rational matrix, with $G(\infty)<\infty$. Let (A,B,C,D) be a minimum realization of G(s). Then G(s) is positive real if and only if there exist real matrices P, Q, R and S such that:

$$PA + A^T P = -Q, \quad B^T P + S^T = C, \quad D + D^T = R \tag{2}$$

where $P > 0$ and $\begin{bmatrix} Q & S \\ S^T & R \end{bmatrix} \geq 0$.

2.2 Strictly Positive Real Systems

Definition 3 [5]: An n×n matrix G(s) is strictly positive real (SPR) if there exists a positive number ε such that $H(s-\varepsilon)$ is positive real.

A system with a strictly positive transfer matrix will be called SPR. In practice, SPR systems are systems that dissipate energy. For such systems, the internal energy generation is strictly negative whenever there exists a non-zero external energy input. Therefore SPR systems are sometimes called dissipative systems. However, the concept of dissipativeness can also be applied to nonlinear systems. Hence SPR systems are dissipative, but the converse is not true. The two notions are equivalent only for the linear time invariant case.

3. NECESSARY AND SUFFICIENT CONDITIONS FOR POSITIVE REALNESS OF SECOND-ORDER SCALAR SYSTEMS

Here we derive necessary and sufficient conditions for the positive realness of scalar second-order scalar systems.

Theorem 3: A scalar second-order system described by

$$m\ddot{x} + c\dot{x} + kx = u \quad \text{and} \quad y = h_a\ddot{x} + h_v\dot{x} + h_d x \tag{3}$$

is PR if and only if

$$\text{(i) } h_a \geq 0, h_v \geq 0, h_d \geq 0 \quad \text{and} \quad \text{(ii)} \left|\sqrt{mh_d} - \sqrt{kh_a}\right| \leq \sqrt{ch_v} \tag{4}$$

Proof: The transfer function of the system in Eq.(3) is

$$G(s) = \frac{h_a s^2 + h_v s + h_d}{ms^2 + cs + k} \tag{5}$$

Conditions 1 and 2 are satisfied. Conditions 3 and 4 are checked in the following. Rewrite Eq.(5):

$$\begin{aligned} \mathrm{Re}[G(j\omega)] &= \left\{mh_a\omega^4 + (-mh_d + ch_v - kh_a)\omega^2 + kh_d\right\} / \left\{(k - m\omega^2)^2 + c^2\omega^2\right\} \\ &= \left\{mh_a\left[\omega^2 + \frac{(-mh_d + ch_v - kh_a)}{2mh_a}\right]^2 - \frac{(-mh_d + ch_v - kh_a)^2}{4mh_a} + kh_d\right\} / \left\{(k - m\omega^2)^2 + c^2\omega^2\right\} \end{aligned} \tag{6}$$

$\mathrm{Re}[G(j\omega)]$ approaches h_a/m when ω approaches infinity. Hence $h_a \geq 0$. For $\omega=0$, we obtain $h_d \geq 0$. Thus we have the following two cases:

$$\begin{aligned} &\text{(a) } h_a \geq 0, h_d \geq 0, \text{and} (-mh_d + ch_v - kh_a) \geq 0 \\ &\text{(b) } h_a \geq 0, h_d \geq 0, \text{and} (-mh_d + ch_v - kh_a) \leq 0 \end{aligned} \tag{7}$$

For Case (a), Equation (6) is positive as seen from the first expression of (6). Note that since $ch_v \geq mh_d + kh_a$, we obtain $ch_v \geq 0$ which implies $h_v \geq 0$. Furthermore, we have $\sqrt{ch_v} \geq \sqrt{mh_d + kh_a}$. For Case (b), since the square term of the numerator can be made equal to zero, we need to check the following inequality:

$$-\frac{(-mh_d + ch_v - kh_a)^2}{4mh_a} + kh_d \geq 0 \tag{8}$$

that is $(\sqrt{mh_d} - \sqrt{kh_a})^2 \leq ch_v \leq mh_d + kh_a$. From the left inequality we have $ch_v \geq 0$, which implies $h_v \geq 0$. Now taking the square roots of the inequality yields

$$\left|\sqrt{mh_d} - \sqrt{kh_a}\right| \leq \sqrt{ch_v} \leq \sqrt{mh_d + kh_a} \tag{9}$$

Combining both cases, we have (i) and (ii) of (4).

The poles of G are the solutions of the equation $ms^2+cs+k=0$. Double imaginary poles are only possible if $c=0$ and $k=0$. However, from (9) we have $h_d=0$. Therefore, the zero pole is simple. As a conclusion, G has no double pole on the imaginary axis. Now it remains to show that the residues of the imaginary poles are real and positive. If $k = 0$, then the residue of the pole at zero is h_v/m, which is real and positive. If $k\neq 0$, G(s) has some poles on the imaginary axis only when $c=0$. The poles are

$j\sqrt{k/m}$ and $-j\sqrt{k/m}$. The residue for the both poles is

$$\text{Re } s = \frac{mh_v j\sqrt{\frac{k}{m}}}{m\,(2mj\sqrt{\frac{k}{m}})} = \frac{h_v}{2m} \geq 0 \tag{10}$$

which is real and positive. Hence the theorem is proved.

4. SUFFICIENT CONDITIONS FOR POSITIVE REALNESS OF SECOND-ORDER MULTIVARIABLE SYSTEMS

In general, a second-order MIMO system can be made positive real by properly choosing the output variables. For the system with velocity and displacement output, a sufficient condition of the positive realness is the collocation of the both outputs with the controller. Moreover, if only velocity output is available, the collocated system is still positive real. The velocity is an important factor of making the system positive real. For example, if only displacement output is available then the system cannot be made positive real. In some space applications, velocity is the most difficult measurement to obtain. Here we discuss conditions for which the system without velocity output can be made positive real.

4.1 Acceleration and Displacement Output

Consider a system represented by

$$M\ddot{x} + D\dot{x} + Kx = Bu \text{ and } y = H_a\ddot{x} + H_d x \tag{11}$$

Assume rank(B)=m, and let $L=B(B^TB)^{-1}$. Furthermore, define $H_a^* = LH_a$ and $H_d^* = LH_d$ and let P be the 2m x 2m matrix

$$P = \begin{bmatrix} H_a^{*T}M & H_a^{*T}K \\ H_d^{*T}M & H_d^{*T}K \end{bmatrix} \tag{12}$$

Theorem 4: If $P \geq 0$, then the system is positive real.

Proof: The input-output scalar product can be expressed as

$$y^Tu = y^TL^TBu = (Ly)^T(Bu) \tag{13}$$

Therefore,

$$\begin{aligned} y^Tu &= (H_a^*\ddot{x} + H_d^*x)^T(M\ddot{x} + D\dot{x} + Kx) \\ &= (H_a^*\ddot{x} + H_d^*x)^TD\dot{x} + (H_a^*\ddot{x} + H_d^*x)^T(M\ddot{x} + Kx) \\ &= \frac{1}{2}\frac{d}{dt}(\dot{x}^TH_a^{*T}D\dot{x} + x^TH_d^{*T}Dx) + (\ddot{x}^T\ x^T)\ P\begin{pmatrix}\ddot{x}\\ x\end{pmatrix} \end{aligned} \tag{14}$$

Therefore, we can define $\lambda(X,u) = (\dot{x}^T\ x^T)\ P\begin{pmatrix}\dot{x}\\ x\end{pmatrix}$. If P is positive semi-definite, then $\lambda(X,u)$ is positive for every X and every u, and hence the system is positive real.

Remark 2: If rank(B)<m, a new input vector u of smaller dimension can be defined, and this input will be such that the new matrix B will have rank m. Thus Theorem 4 can be applied in general cases.

The following theorem can be applied to make P positive semidefinite.

Theorem 5: P is positive definite if and only if

$$B(B^TB)^{-1}H_aM^{-1} \geq 0 \text{ and } H_d = H_aM^{-1}K \tag{15}$$

Proof: Assume that P is positive semi-definite. Since M is nonsingular, there exists a positive real number k such that the matrix $H_a^* + kM$ is non-singular. For such a k assume that the matrix $E = K - M(H_a^* + kM)^{-1}(H_d^* + kK)$ is not equal to zero. Then there exists a vector x_2 such that Ex_2 is not zero. Define $x_1 = -(H_a^* + kM)^{-1}(H_d^* + kK)\,x_2$. As a consequence, if $X = (x_1^T\ x_2^T)^T$, we have $X^TP\,X = -k\,\|Mx_1 + Kx_2\|^2 = -k\,\|Ex_2\|^2$ which is strictly negative. This is impossible. As a consequence, E must be equal to zero , i.e. $K = M(H_a^* + kM)^{-1}(H_d^* + kK)$. Multiplying through this equality by $(H_a^* + kM)M^{-1}$ yields $H_a^*M^{-1}K = H_d^*$. Thus,

$$(x_1^T \; x_2^T)\, P \begin{pmatrix} x_1 \\ x_2 \end{pmatrix} = (Mx_1 + Kx_2)^T M^{-1} H_a^{*T} (Mx_1 + Kx_2) \tag{16}$$

Since x_1 and x_2 can be chosen arbitrarily, another necessary condition is that the matrix $M^{-1}H_a^{*T}$ be positive semidefinite. Hence necessary conditions for positive semidefiniteness of P are

$$M^{-1}H_a^{*T} \geq 0 \text{ and } H_d^* = H_a^* M^{-1} K \tag{17}$$

Those two conditions are clearly also sufficient conditions. Conditions (17) can be rewritten using the initial matrices:

$$B(B^TB)^{-1}H_a M^{-1} \geq 0 \text{ and } H_d = H_a M^{-1} K \tag{18}$$

Combining Theorems 4 and 5 leads to the following theorem.

Theorem 6: If conditions (18) are satisfied, then the system represented by Equations (11) is positive real.

Remark 3: The conditions stated in Theorem 6 are necessary and sufficient in the scalar case. They can be compared to conditions (4) with h_v=0.

4.2 Displacement Output with Feed-Forward Loop

In Theorem 6 if no exact values of the matrices M and K are known, then the theorem cannot be implemented. In this case the following theorem can be used instead.

Theorem 7: Assume that the system is represented by

$$M\ddot{x} + D\dot{x} + Kx = Bu \text{ and } y = H_d x + J u \tag{19}$$

where K > 0, D > 0, and J is an m x m matrix. Then there exists a positive real number η such that the system is positive real when

$$H_d = \alpha_2 B^T \text{ and } J = \beta B^T B \tag{20}$$

with $a_2 > \eta$ and $b \geq \alpha_2^2 / 2$.

Proof: The idea here is that u is a function of $M\ddot{x} + D\dot{x} + Kx$. Therefore u includes information on the velocity $\dot{x}$ and adding u to the system output makes the system positive real. Furthermore, the input u is measurable in many applications. The system is represented by the following equations:

$$\begin{cases} \dot{X} = AX + B_2 u \\ Y = CX + D u \end{cases} \tag{21}$$

where $A = \begin{bmatrix} 0 & I \\ -M^{-1}K & -M^{-1}D \end{bmatrix}$, $B_2 = \begin{bmatrix} 0 \\ M^{-1}B \end{bmatrix}$, $C = \begin{bmatrix} H_d & 0 \end{bmatrix}$ and $D = J$. Here we use the K-Y Lemma. To make $\begin{bmatrix} Q & S \\ S^T & R \end{bmatrix}$ positive semi-definite, let us choose $Q \geq I$ and $R \geq SS^T$. Let $P_1 = \alpha_2 K + \alpha_3 D$, $P_2 = \alpha_2 M$ and $P_3 = \alpha_3 M$. This yields

$$Q = \begin{bmatrix} 2\alpha_3 K & 0 \\ 0 & 2\alpha_2 D - 2\alpha_3 M \end{bmatrix} \tag{22}$$

Since K>0, there exists a $\xi = \xi(K)$ such that $\alpha_3 > \xi$ which implies $Q_1 = 2\alpha_3 K \geq I$. For $\alpha_3 = \alpha_{3_0} > \xi$, as D > 0, there also exists a positive number $\eta_0(\alpha_3, D, M)$ such that $\alpha_2 \geq \eta_0$ which implies $Q_2 = 2\alpha_2 D - 2\alpha_3 M \geq I$.. Therefore $Q \geq I$.. Now we want to have $R = D + D^T \geq SS^T$. Let

$$S = C^T - PB_2 = \begin{bmatrix} H_d^T - \alpha_3 B \\ -\alpha_2 B \end{bmatrix} \tag{23}$$

Let $H_d = \alpha_3 B^T$. Then $S^T S = \alpha_2^2 B^T B$. Therefore, we must have $D + D^T \geq \alpha_2^2 B^T B$. Select $D = \beta B^T B$ and β such that $D + D^T = 2\beta B^T B \geq \alpha_2^2 B^T B$. This is satisfied whenever $\beta \geq \alpha_2^2 / 2$. Finally P must be positive definite. Since M>0, we can find a positive number $\eta_1(\alpha_{3_0}, M, K, D)$ such that $\alpha_2 > \eta_1$ which implies P>0. To finish the proof, let $\eta = \max(\eta_0, \eta_1)$.

5. CONTROL OF POSITIVE REAL SECOND-ORDER SYSTEMS

Consider the following feedback control scheme for the plant

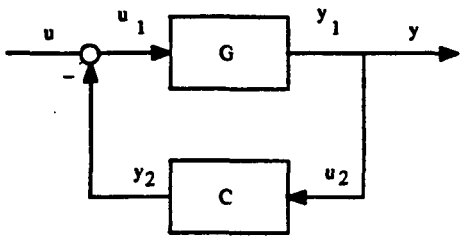

Fig. 1

It is easy to show that the closed-loop is positive real if G and C are positive real. Hence the closed-loop system is stable, but not necessarily strictly stable. Its transfer matrix may have some poles on the imaginary axis. As a consequence, the output of the system will not necessarily converge to zero when u=0. If the systems G and C are strictly positive real, the closed-loop system is strictly positive real and therefore strictly stable. In this case y will go to zero when t gets large. Still this result is not very useful in practise since it might not be possible to make the plant G strictly positive real in a real application. A very interesting theorem stated in [4] is the following.

Theorem 8 [4] : If in the feedback system of Fig. 1 G(s) and C(s) are square transfer matrices, then the closed-loop system is asymptotically stable in the input/output sense if G is PR and if C is SPR.

Our control objective is to have $\lim_{t\to\infty} x = 0$ when u=0. With a certain class of controllers, it can be proved that this objective is achieved. This result is stated in the following theorem.

Theorem 9 : If the transfer matrix of the controller is constant and positive definite, then $\lim_{t\to\infty} x = 0$ when u=0.

Proof: The system is represented by the following equations:

$$\begin{cases} (M + BCH_a)\ddot{x} + (D + BCH_v)\dot{x} + (K + BCH_d)x = Bu \\ y = H_a\ddot{x} + H_v\dot{x} + H_d x \end{cases} \tag{24}$$

Let

$$M + BCH_a = M^*,\ D^* = D + BCH_v \text{ and } K^* = K + BCH_d \tag{25}$$

The representation of the plant with first-order dynamic equations is now

$$\begin{cases} \dot{X} = AX + Bu \\ y = CX + Du \end{cases} \tag{26}$$

where $X=\begin{bmatrix} x \\ \dot{x} \end{bmatrix}$, and $A = \begin{bmatrix} 0 & I \\ -M^{*-1}K^* & -M^{*-1}D^* \end{bmatrix}$. M^* will always be non-singular when the output of the system to be controlled is designed with the method in Section 4. Furthermore, this representation will be minimal for our applications. If u=0, we have $\dot{X} = AX$. Since the system is stable, all the eigenvalues of A have strictly negative real parts. As a consequence, $\lim_{t\to\infty} X = 0$. This means that $\lim_{t\to\infty} x = 0$ and $\lim_{t\to\infty} \dot{x} = 0$.

6. EXAMPLE

Consider spring-mass-dashpot system shown in Fig.2.

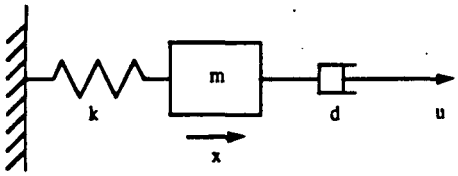

Fig. 2

The system is governed by:

$$m\ddot{x} + d\dot{x} + kx = u \tag{27}$$

The parameters m, k and d are not known precisely. Assume that $2\le m\le 4$, $4<d<6$ and $1<k<3$. We will design an output y that makes the system positive real regardless of the uncertainty on its parameters. Theorem 7 can be used here, since m, d and k are

always strictly positive. First $2\alpha_3 k \geq 1$ must be chosen. If $\alpha_3 \geq 1/(2k_{min})$, then this condition will be satisfied for $k \in [1, 3]$. Let $\alpha_3 = 1/2$. Next we want to have $\alpha_2 d \geq (m+1)/2$. If $\alpha_2 \geq (m_{max}+1)/(2d_{min})$, then this condition will be satisfied for $m \in [2, 4]$ and $d \in [4, 6]$. Hence we select $\alpha_2 \geq 5/8$. Now the other condition is $\alpha_2 k \geq \alpha_3^2 m^2 - \alpha_3 d$, i.e. $\alpha_2 \geq (m^2 - 2d)/(4k)$. This condition is satisfied if $\alpha_2 \geq (m_{max}^2 - 2d_{min})/(4k_{min})$. Since $(m_{max}^2 - 2d_{min})/(4k_{min}) = \frac{8}{4} = 2$, this condition is reduced to $\alpha_2 \geq 2$. Therefore, a general constraint on α_2 is $\alpha_2 \geq 2$. A possible choice is $\alpha_2 = 2$. Finally a number $\beta \geq \alpha_2^2/2$ must be chosen. $\beta = 2$ is a possible choice. As a conclusion, the output of the system is $y = 2x + 2u$. The system is robustly positive real with this choice. Any constant controller will stabilize the state x of the system.

7. CONCLUSIONS

In this paper, necessary and sufficient conditions for positive realness of second-order SISO systems have been derived. In the MIMO case, two designs using different choices of output variables have been presented for the system without velocity output. Finally a possible control method for such systems has been examined, illustrated by the simple example.

REFERENCES

Papers:

[1] J-N. Juang and M. Phan, Robust Controller Designs for Second-order Dynamic Systems: A Virtual Approach, NASA Technical Memorandum TM-102666, May 1990.

[2] J-N. Juang, S-C. Wu, M. Phan, and R.W. Longman, Passive Dynamic Controllers for Nonlinear Mechanical Systems, NASA Technical Memorandum 104047, March 1991.

[3] D.D. Siljak, New Algebraic Criteria for Positive Realness, in Journal of Franklin Institute, vol. 291, NO. 2, February 1971, pp 109-120.

[4] R.J. Benhabib, R.P. Iwens and R.L. Jackson, Stability of Large Structure Control Systems Using Positivity Concepts, in Journal of Guidance and Control, vol. 4, NO. 5, SEPT.-OCT. 1981.

Books:

[5] Y. D. Landau, Adaptive Control, the Model Reference Approach, 1979.

AIAA-93-3806-CP

A ROBUST CONTROLLER FOR SECOND-ORDER SYSTEMS USING ACCELERATION MEASUREMENTS

C.-H. Chuang[1] and Oliver Courouge[2]
Georgia Institute of Technology, Atlanta, GA 30332
and
Jer-Nan Juang[3]
NASA Langley Research Center, Hampton, VA 23665

ABSTRACT

This paper presents a robust control design using strictly positive realness for second-order dynamic systems. The robust strictly positive real controller allows the system to be stabilized with only acceleration measurements. An important property of this design is that stabilization of the system is independent of the system parameters. The control design connects a virtual system to the given plant. The combined system is positive real regardless of system parameter uncertainty. Then any strictly positive real controllers can be used to achieve robust stability. A spring-mass system example and its computer simulations are presented to demonstrate this controller design. Robust performance property of this design is also demonstrated in a simple example.

1. INTRODUCTION

Positive real (PR) systems have many applications for shape and vibration control of large flexible structures. In most of those PR designs, the output of the plant is usually assumed to include velocity, and the sensors are assume to be collocated with the actuators. In [1], position and velocity feedback are used together to control large space structures, and the controllers are strictly positive real. PR feedback with velocity measurement is examined in [2] for control of a flutter mode. [3] presents a robust multivariable control of structures using a passive controller in which the velocity sensors are collocated with the control actuators. Several passive control designs using acceleration, velocity and position measurements are presented in [4]. [5] generalizes the designs in [4] to handle nonlinear systems. The method presented in [6] uses displacement sensors. Similarly, [7] examines direct position plus velocity feedback. A feedforward positive real design can be seen from [11].

Nevertheless, in some application areas, only acceleration is directly measurable. Even though velocity and position can be obtained by integrating the measured acceleration, exact initial values of velocity and position are needed to achieve asymptotic stability. The bias in acceleration measurement can also decreases the integration accuracy. In this study we develop a virtual system which is connected to a strictly positive real (SPR) controller for multivariable second-order system when only acceleration is directly measurable. Although integration is carried out in the virtual system, initial values of the the states of the virtual system can be arbitrary and the closed-loop system is asymptotically stable. Furthermore, the bias in acceleration measurement can be scaled down by the system matrix of the virtual system. Since any SPR controllers can be connected to the virtual system, the controller design here is different from an integral control.

In this paper, we review some definitions and a theorem associated with dissipativeness and passivity. Dissipativeness and passivity are then related to strictly positive realness and positive realness. Using these backgrounds we develop a virtual system to compute an output which will make the combined system of the plant with the virtual system positive real. The inputs to the virtual system are only acceleration and the control force applied to the plant. More important, the virtual system is model independent, and thus the global system is robustly positive real. Therefore an input/output controller can be constructed by using any strictly positive real controllers. When the stiffness matrix of the second-order system is positive definite, we show that it is possible to stabilize the displacement if the actuators are properly located. With this design, the displacement is globally asymptotically stable. A spring-mass example with three masses and no damping is used to illustrate our design method. Robust performance is demonstrated for a spring-mass system with only one mass and one spring. Computer simulations are also presented.

2. PRELIMINARIES

The concept of dissipativeness describes an important input-ouput property of dynamical systems. Consider a system with input u and output y, where u is an m×1 vector and y is a p×1 vector. A supply rate for the system is defined as follows.

Definition 1 [8]: A supply rate is a real function of u and y defined as

$$w(u,y) = y^T Q y + 2 y^T S u + u^T R u \qquad (1)$$

1. School of Aerospace Engineering, Assistant Professor, AIAA Senior Member
2. School of Aerospace Engineering, Graduate Research Assistant
3. Spacecraft Dynamics Branch, Principal Scientist, AIAA Fellow

where Q, S, and R are any constant real matrices with dimensions p×p, p×m and m×m respectively.

Q and R are usually symmetric matrices, and w(u,y) is often called the input energy into the system. Dissipativeness is defined with respect to the supply rate w(u,y) in the following definition.

Definition 2 [8]: The system with input u and output y is called dissipative with respect to the supply rate w(u,y) if for all locally integrable u(t) and all $T \geq t_0$, we have

$$\int_{t_0}^{T} w(t)\,dt \geq 0 \tag{2}$$

where $x(t_0)=0$ and where $w(t)=w(u(t),y(t))$ which is evaluated along the trajectory of the system interested.

Eq.(2) means that an initially unexcited system can only absorb energy as long as the system is dissipative. If the supply rate represents the input energy into the system, then Eq.(2) states that a system with no initially stored energy transforms the input energy into either stored energy or dissipated energy. Thus no energy can be generated from a dissipative system. Note that the dissipative system defined by (1) and (2) are not necessary the systems which "dissipate" energy by a usual sense.

Passivity is defined as a special case of dissipativeness defined by (1) and (2).

Definition 3 [8]: A system is passive if and only if it is dissipative with respect to the supply rate

$$w(u,y) = u^T y \tag{3}$$

An algebraic condition for passivity can be found if the system is represented by the state-space equations

$$\begin{aligned} \dot{x} &= f(x) + G(x)u \\ y &= h(x) + J(x)u \end{aligned} \tag{4}$$

where f(x) and h(x) are real vector functions of the state vector x, with f(0)=0, h(0)=0, and G(x) and J(x) are real matrix functions of x. These four functions are assumed to be infinitely differentiable. We also assume that u and y have the same dimension. The system is furthermore assumed to be completely controllable. Theorem 1 provides a test for the passivity of a system written in the form of Eq. (4).

Theorem 1 [9]: The system is passive if and only if there exist real functions f(x), l(x) and W(x) with $\phi(x)$ continuous and with

$$\phi(x) \geq 0, \quad \forall x \in R^n \tag{5}$$

and

$$\phi(0) = 0 \tag{6}$$

such that

$$\begin{aligned} &\text{(i)} \quad \nabla^T \phi(x) f(x) = -l^T(x) l(x) \\ &\text{(ii)} \quad \frac{1}{2} G^T(x) \nabla \phi(x) = h(x) - W^T(x) l(x) \\ &\text{(iii)} \quad J(x) + J^T(x) = W^T(x) W(x), \quad \forall x \in R^n \end{aligned} \tag{7}$$

Moreover, if J (x) is a constant matrix, then W(x) may be taken to be constant.

The function f(x) is generally not unique for a given passive system. Nevertheless, the function $\phi(x)$ has a physical meaning which is shown in [9] that

$$\begin{aligned} 2\int_{t_0}^{T} u^T(t) y(t)\,dt &= \phi[x(T)] - \phi[x(t_0)] \\ &+ \int_{t_0}^{T} [l(x) + W(x)u]^T [l(x) + W(x)u]\,dt \end{aligned} \tag{8}$$

Eq.(8) may be interpreted as the conservation of energy equation. $\frac{1}{2}\phi(x)$ is a stored energy for the system. The left-hand side integral of Eq. (8) corresponds to the input energy to the dynamic system. The right-hand integral is proportional to dissipated energy, and it is always non-negative. As a consequence, Eq.(8) means that the energy input is equal to the variation of stored energy plus the loss of energy which is a positive function.

A linear system is passive if and only if its transfer matrix is positive real [10]. Passivity can thus be seen as a generalization of positive realness for nonlinear systems. Since the systems investigated here are linear, we will equivalently use these two concepts for the rest of this paper.

3. A VIRTUAL SYSTEM DESIGN

The multivariable system (Plant (P)) is described by

$$M\ddot{x} + D\dot{x} + Kx = Bu \tag{9}$$

where u is an m×1 control vector, x is an n×1 state vector, M is an n×n symmetric positive definite matrix, D and K are n×n symmetric positive semi-definite matrices, and B is an n×m matrix. Let a virtual system (V) be defined by the following equation

$$\ddot{x}_a = A\ddot{x} + B'u \tag{10}$$

where L is a p×n matrix, B' is a p×m matrix, and x_a is a p×p vector. The following theorem allows us to compute an output y that will make the global system (a combined

system of the given plant and the virtual system) positive real. Note that since Λ has p×n dimensions, the number of state variables for the virtual system x_a can be made smaller than the number of the plant state variables x.

Theorem 2: Let H_v, Λ be chosen such that

$$\begin{aligned} 2H_v\Lambda &= B^T \\ B^T M_a^T &= 2H_v \end{aligned} \tag{11}$$

where M_a is a p× p positive semi-definite matrix. If

$$y = H_v \dot{x}_a \tag{12}$$

then the system with input u and output y is positive real.

This scheme is illustrated in Fig. 1

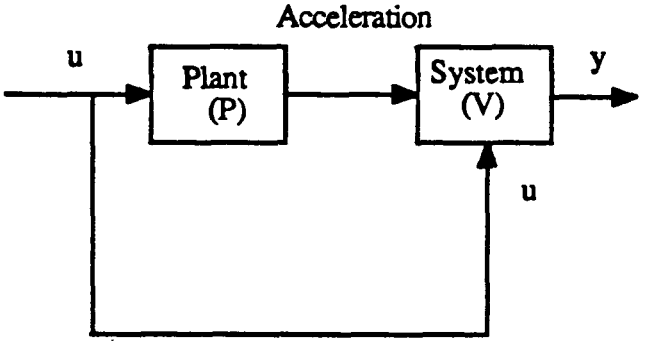

Figure 1. A Virtual System

Proof: For this proof, it is useful to represent the system with a state-space representation. Let

$$X^T = [x_1^T\ x_2^T\ x_3^T\ x_4^T] = [x^T\ \dot{x}^T\ x_a^T\ \dot{x}_a^T] \tag{13}$$

The equations describing the global system may be rewritten as

$$\begin{cases} \dot{X} = f(X) + G(X)u \\ Y = h(X) + J(X)u \end{cases} \tag{14}$$

where

$$f(X) = \begin{bmatrix} x_2 \\ -M^{-1}Dx_2 - M^{-1}Kx_1 \\ x_3 \\ -\Lambda M^{-1}Dx_2 - \Lambda M^{-1}Kx_1 \end{bmatrix} \tag{15}$$

$$G(X) = \begin{bmatrix} 0 \\ M^{-1}B \\ 0 \\ \Lambda M^{-1}B + B \end{bmatrix} \tag{16}$$

$$h(X) = \begin{bmatrix} 0 \\ 0 \\ 0 \\ H_v x_4 \end{bmatrix} \tag{17}$$

$$J(X) = 0 \tag{18}$$

Let a candidate for the function f(X) in Theorem 2 be

$$\phi(X) = \frac{1}{2}\dot{x}^T M\dot{x} + \frac{1}{2}x^T Kx + \frac{1}{2}(\dot{x}_a - \Lambda\dot{x})^T M_a(\dot{x}_a - \Lambda\dot{x}) \tag{19}$$

where M_a is positive semi-definite. The sum of the first two terms corresponds to the stored energy of the plant. The third term is added to achieve a positive real design. The function f(X) can be written using the state variables as

$$\phi(X) = \frac{1}{2}x_2^T M x_2 + \frac{1}{2}x_1^T K x_1 + \frac{1}{2}(x_4 - \Lambda x_2)^T M_a(x_4 - \Lambda x_2) \tag{20}$$

f(X) is a positive function and f(0)=0. It must be checked that there exists a function l (X) such that

$$\nabla^T\phi(X)f(X) = -l^T(X)l(X) \tag{21}$$

This calculation is considerably simplified when we notice that

$$\nabla^T\phi(X)f(X) = \left.\frac{d\phi(X)}{dt}\right|_{u=0} \tag{22}$$

As a consequence we have

$$\begin{aligned} \nabla^T\phi(X)f(X) &= \dot{x}^T(M\ddot{x} + Kx) \\ &+ \frac{1}{2}(\ddot{x}_a - \Lambda\ddot{x})^T M_a(\dot{x}_a - \Lambda\dot{x}) + \frac{1}{2}(\dot{x}_a - \Lambda\dot{x})^T M_a(\ddot{x}_a - \Lambda\ddot{x}) \Big|_{u=0} \end{aligned} \tag{23}$$

When u = 0, the last two terms cancel out and therefore

$$\nabla^T\phi(X)f(X) = \dot{x}^T(M\ddot{x} + Kx)\Big|_{u=0} \tag{24}$$

Thus we finally have

$$\nabla^T\phi(X)f(X) = -\dot{x}^T D\dot{x} = -x_2^T Dx_2 \tag{25}$$

Since D is positive semi-definite, it is possible to find a matrix R such that $D=R^TR$. The above equality becomes

$$\nabla^T\phi(X)f(X) = -(Rx_2)^T(Rx_2) = -l^T(X)l(X) \tag{26}$$

where $l(X)=Rx_2$. Thus equality (i) from Theorem 1 is satisfied. Equality (iii) of Eq. (7) reduces to

$$J(X)+J^T(X)=W^T(X)W(X)=0 \tag{27}$$

The function W(X) is therefore equal to zero. Equality (ii) of Eq. (7) becomes

$$h(X)=\frac{1}{2}G^T(X)\nabla\phi(X) \tag{28}$$

Since the first and third rows of G(x) are zero, only the partial derivatives with respect to velocity are needed to evaluate Eq. (28). Therefore, we have

$$\begin{aligned}\frac{\partial\phi}{\partial x_2}&=x_2^T M+(\Lambda x_2-x_4)^T M_a \Lambda\\ \frac{\partial\phi}{\partial x_4}&=(x_4-\Lambda x_2)^T M_a\end{aligned} \tag{29}$$

The function h(X) is such that

$$2h(X)=(M^{-1}B)^T\left(\frac{\partial\phi}{\partial x_2}\right)^T+(\Lambda M^{-1}B+B')^T\left(\frac{\partial\phi}{\partial x_4}\right)^T \tag{30}$$

Obvious simplifications yield

$$2h(X)=(B^T-B^T M_a^T\Lambda)x_2+B^T M_a^T x_4 \tag{31}$$

h(X) is equal to $H_v x_4$ if the following equations are satisfied

$$\begin{aligned}B^T-B^T M_a^T\Lambda&=0\\ B^T M_a^T&=2H_v\end{aligned} \tag{32}$$

Those equations can be rewritten as

$$\begin{aligned}2H_v\Lambda&=B^T\\ B^T M_a^T&=2H_v\end{aligned} \tag{33}$$

and the theorem is proved •

There are several possible ways to solve the above system of equations. Given H_v and B, we can solve for some possible L, M_a and B'. At the end of the calculation, it must be checked that M_a is positive semi-definite. Another method consists of choosing B, L and a positive semi-definite M_a and then solving for possible B' and H_v. Note that the choice of the virtual system in Eq. (10) is independent of the plant parameter M, D, and K. This means that the virtual system will make the global system positive real regardless the uncertainty in M, D, and K.

4. CHOICE OF A CONTROLLER

If the output of the global system is chosen according to Theorem 2, then the global system is positive real. Thus the closed-loop system is uniformly asymptotically stable with zero input if the controller is strictly positive real [3]. That is, for this case, we have

$$\lim_{t\to\infty}(H_v\dot{x}_a)=0 \tag{34}$$

Our next goal is to let x go to zero. Theorem 3 may be used to achieve this goal.

Theorem 3: Assume that Theorem 2 is used to make the global system PR. Furthermore assume that

(i) $B^T\bar{x}=0$ and $u=0$ imply $\bar{x}=0$.

(ii) K is positive definite.

(iii) The system is connected to a SPR closed-loop controller.

Then $\lim_{t\to\infty}x(t)=0$.

Fig.2 shows the control scheme for the plant (P) and virtual system (V).

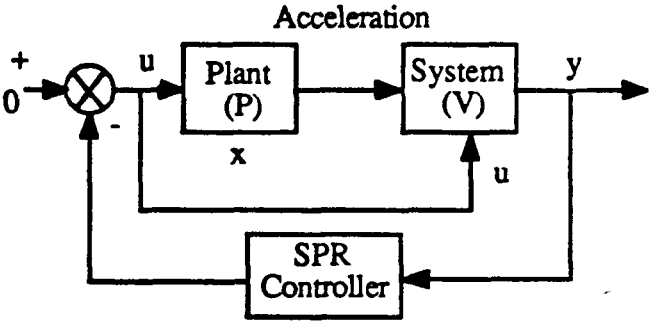

Figure 2. A SPR Controller for the plant and the Virtual System

Theorem 3 allows us to design a robust controller for Plant (P). No knowledge of the constant matrices M, D and K is required. Furthermore, the only measurements needed are acceleration and input. Acceleration may easily be measured for many practical systems by using accelerometers. The input u may be obtained by measuring the output of the SPR controller.

The proof of Theorem 3 uses the following lemma.

Lemma 1: Let $\varepsilon(t)$ be a function of time and let $\varepsilon(t)$ go to zero as time increases. Then if x satisfies the differential equation

$$D\dot{x}+Kx=\varepsilon \tag{35}$$

where D is positive semi-definite and K is positive definite, then x converges to zero.

Proof: Let m denote the rank of D. There exists an invertible n×n matrix P such that

$$D^* = P\,D\,P^{-1} \tag{36}$$

where

$$D^* = \begin{bmatrix} 0 & 0 \\ 0 & D_{22} \end{bmatrix} \tag{37}$$

Note that since D is positive semi-definite, the aero eigenvalues appear on D^*. P is an orthogonal matrix consisting of the eigenvalues of D matrix. Therefore, D_{22} is an m×m positive definite matrix. Let K^* be defined as

$$K^* = P\,K\,P^{-1} \tag{38}$$

K^* may be written as

$$K^* = \begin{bmatrix} K_{11}^* & K_{12}^* \\ K_{21}^* & K_{22}^* \end{bmatrix} \tag{39}$$

The dynamical equation can be written as

$$PDP^{-1}(P\dot{x}) + PKP^{-1}(Px) = P\varepsilon(t) \tag{40}$$

Let $y = Px$ and $\eta(t) = P\varepsilon(t)$. The system is now described by

$$D^*\dot{y} + K^* y = \eta(t) \tag{41}$$

Let $y = \begin{pmatrix} y_1 \\ y_2 \end{pmatrix}$ and $\eta = \begin{pmatrix} \eta_1 \\ \eta_2 \end{pmatrix}$. Eq. (41) is reduced to

$$\begin{cases} K_{11}^* y_1 + K_{12}^* y_2 = \eta_1(t) \\ D_{22}\dot{y}_2 + K_{21}^* y_1 + K_{22}^* y_2 = \eta_2(t) \end{cases} \tag{42}$$

The first equation of (42) can be solved in terms of y_1, and Eq. (45) reduces to

$$\begin{cases} y_1 = -K_{11}^{*-1} K_{12}^* y_2 + K_{11}^{*-1}\eta_1(t) \\ D_{22}\dot{y}_2 + (K_{22}^* - K_{21}^* K_{11}^{*-1} K_{12}^*) y_2 = \eta_2(t) + K_{21}^* K_{11}^{*-1}\eta_1(t) \end{cases} \tag{43}$$

Note that since K is positive definite, K_{11}^* is invertible. D_{22} and $(K_{22}^* - K_{21}^* K_{11}^{*-1} K_{12}^*)$ are positive definite matrices. Thus y_2 may be considered as the output of a strictly stable system. The output of the strictly stable system converges to zero. The parameter y_2 will therefore go to zero. The first equality in Eq.(43) shows that y_1 also goes to zero. Consequently, y converges to zero and so does x.

Proof of Theorem 3: Refer to Fig.2, (-u) is the output of the SPR controller. Since a SPR controller is always strictly stable, when y goes to zero, u also goes to zero. Furthermore, we have

$$2H_v\ddot{x}_s = 2H_v\Lambda\dot{x} + 2H_v B'\dot{u} \tag{44}$$

by multiplying Eq.(10) with $2H_v$. Since $2H_v\Lambda = B^T$, this equation may be rewritten as

$$B^T\ddot{x} = 2H_v\ddot{x}_s - 2H_v B'\dot{u} \tag{45}$$

$2H_vB'u$ goes to zero as u goes to zero. Furthermore, we know that $y = H_v\dot{x}_s$ converges to zero as time increases.

Let x_c denote the state of the SPR controller. Since the controller is linear, the system can be described by

$$\begin{aligned} \dot{x}_c &= Rx_c + Sy \\ y_c &= Tx_c \end{aligned} \tag{46}$$

where R, S, and T are constant matrices. Therefore, the global system becomes

$$\begin{aligned} M\ddot{x} + B\dot{x} + Kx &= -BTx_c \\ \dot{y} &= (H_v\Lambda)\dot{x} - (H_vB'T)x_c \\ \dot{x}_c &= Rx_c + Sy \end{aligned} \tag{47}$$

Further define $x = [x^T\ \dot{x}^T\ x_c^T\ y^T]^T$. Eq. (47) is rewritten in the form

$$\dot{x} = Ax \tag{48}$$

where

$$A = \begin{bmatrix} 0 & 1 & 0 & 0 \\ -M^{-1}K & -M^{-1}B & -M^{-1}B^T & 0 \\ 0 & 0 & R & S \\ 0 & H_v\Lambda & -H_vB'T & 0 \end{bmatrix} \tag{49}$$

Since A is constant, the solution for y can be rewritten as

$$y = \sum_i \alpha_i e^{(a_i + j\beta_i)t} p_i(t) \tag{50}$$

where α_i are complex constants and

$$p_i(t) = \sum_{i=1}^{n} \beta_i t^{i-1} \tag{51}$$

Note that n is the number of dimension of matrix A. Since $\lim_{t\to\infty} y(t) = 0$, $a_i < 0$ for all i. Therefore,

$$\lim_{t\to\infty}\frac{dy}{dt}=\lim_{t\to\infty}\{\sum_i \alpha_i(a_i+jb_i)e^{(a_i+jb_i)x}p_i(t) + \sum_i \alpha_i e^{(a_i+jb_i)x}\frac{dp_i(t)}{dt}\}=0 \quad (52)$$

As a consequence, $B^T\ddot{x}$ goes to zero. The equations describing the system are linear and consequently continuous. Thus, if $B^T\ddot{x}$ and u go to zero, $\ddot{x}$ goes to zero according to assumption (i) in Theorem 3. The dynamics of the closed-loop system is now

$$D\dot{x}+Kx=Bu-M\ddot{x}=\varepsilon(t) \quad (53)$$

where $\varepsilon(t)$ vanishes as time increases. Using Lemma 1 we conclude that x (t) goes to zero.

5. EXAMPLES

Two spring-mass systems will be used to demonstrate the controller design.

The first example is a system with three masses, three springs and no dashpots. The example is shown in Fig. 3.

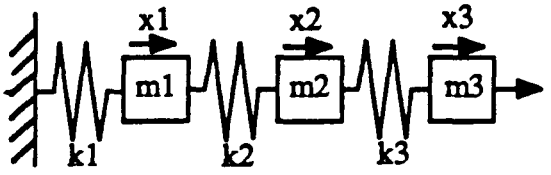

Figure 3. A Spring-Mass System

This system needs to be stabilized as it is not naturally asymptotically stable. With no control and non-zero initial conditions, the three masses oscillate since there is no damping. The dynamic equations describing the system in Fig.3 are

$$\begin{cases} m_1\ddot{x}_1+(k_1+k_2)x_1-k_2x_2=u_1 \\ m_2\ddot{x}_2-k_2x_1+(k_2+k_3)x_2-k_3x_3=u_2 \\ m_3\ddot{x}_3-k_3x_2+k_3x_3=u_3 \end{cases} \quad (54)$$

The matrices M, D and K are

$$M=\begin{bmatrix} m_1 & 0 & 0 \\ 0 & m_2 & 0 \\ 0 & 0 & m_3 \end{bmatrix} \quad (55)$$

$$D=0 \quad (56)$$

$$K=\begin{bmatrix} k_1+k_2 & -k_2 & 0 \\ -k_2 & k_2+k_3 & -k_3 \\ 0 & -k_3 & k_3 \end{bmatrix} \quad (57)$$

M and K are positive definite as long as none of the masses and the spring constants is equal to zero. Several possible controller designs can be used here. Although we select m=p in the following example, $m\neq p$ is allowed for this controller design.

m=n=p=3

There are three control parameters here. A reasonable choice is

$$B=\begin{bmatrix} 1 & 0 & 0 \\ 0 & 1 & 0 \\ 0 & 0 & 1 \end{bmatrix} \quad (58)$$

and the control vector u is defined by $u^T=[u_1\ u_2\ u_3]$. Obvious solutions to Eq.(11) are given by

$$\begin{aligned} \Lambda &= I_{3\times3} \\ H_v &= \frac{1}{2}B^T \\ B' &= \lambda B \\ M_a &= \frac{1}{\lambda}I_{3\times3} \end{aligned} \quad (59)$$

where λ is an arbitrary strictly positive real number. As a consequence, the virtual state vector x_a is generated by the differential equation

$$\ddot{x}_a=\ddot{x}+\lambda Bu \quad (60)$$

All the assumptions of Theorem 3 are satisfied. The vector x may therefore be controlled with the help of any SPR feedback controller. A simple choice is a constant controller, that is a controller with a transfer matrix of the form k I, where I is the identity matrix and k is a constant.

The following values are used in the simulation:

$$m_1=m_2=m_3=1 \quad (61)$$

$$k_1=1 \quad k_2=2 \quad k_3=3 \quad (62)$$

The initial conditions are arbitrarily chosen to be

$$x_1(0)=5 \quad x_2(0)=-2 \quad x_3(0)=9 \quad (63)$$

$$\dot{x}_1(0)=3 \quad \dot{x}_2(0)=5 \quad \dot{x}_3(0)=-4 \quad (64)$$

For the vector x_a, we choose the simple initial conditions

$$x_a=0 \quad \dot{x}_a=0 \quad (65)$$

The constant λ is selected to be 0.5. The gain of the feedback controller is k =1. The three displacements of the three masses are shown in Fig. 4. In the following figures, x_1 is indicated by ——, x_2 is indicated by ··· and x_3 is indicated by – – –.

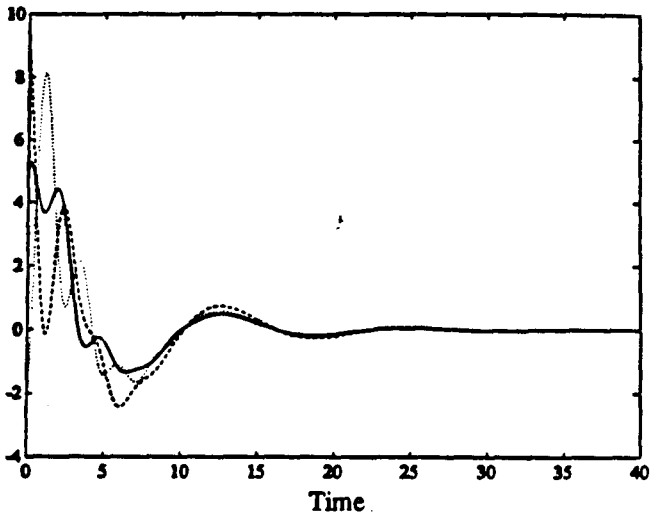

Figure 4 Displacements of x_1, x_2, and x_3

The control goal is achieved since the three displacements vanish with time. Nevertheless, this design requires that a force be applied to each masses. It is possible to reduce the number of actuators with the following control designs.

<u>m=p=2</u>

Here only two forces are applied to the system. Thus there are three possible choices, depending on what masses the forces are applied. Let us assume

$$B=\begin{bmatrix}1 & 0\\ 0 & 1\\ 0 & 0\end{bmatrix} \tag{66}$$

This choice means that the forces are applied to the masses m_1 and m_2 only. The control vector u is is$u^T=[u_1 \quad u_2]$. The vector x_a is now a vector with dimension 2. Eq.(11) has the following solution

$$\begin{aligned}\Lambda &= B^T\\ H_v &= \frac{1}{2}I_{2\times 2}\\ B' &= \lambda I_{2\times 2}\\ M_a &= \frac{1}{\lambda}I_{2\times 2}\end{aligned} \tag{67}$$

where λ is an arbitrary strictly positive real number , and where I denotes the 2×2 identity matrix. Thus x_a can be computed from the following differential equation.

$$\begin{bmatrix}\ddot{x}_{a1}\\ \ddot{x}_{a2}\end{bmatrix}=\begin{bmatrix}\bar{x}_1\\ \bar{x}_2\end{bmatrix}+\lambda\begin{bmatrix}u_1\\ u_2\end{bmatrix} \tag{68}$$

and the output of the system is $y=\frac{1}{\lambda}\dot{x}_a$. In this example, the number of the virtual states is less than the number of the plant states.

A SPR controller must be chosen to control the system. Here again, a constant controller is a possible choice. Its transfer matrix is k I, where k is a positive constant.

It remains to ensure that $B^T\bar{x}=0$ and u=0 imply x=0. If $B^T\bar{x}=0$ and u=0, then the dynamical equations of the system become

$$\begin{cases}(k_1+k_2)x_1+k_2x_2=0\\ -k_2x_1+(k_2+k_3)x_2-k_3x_3=0\\ m_3\ddot{x}_3-k_3x_2+k_3x_3=0\end{cases} \tag{69}$$

By differentiating the second equation and solving for $\ddot{x}_3$, we have

$$\ddot{x}_3=-\frac{k_2}{k_3}\bar{x}_1+\frac{(k_2+k_3)}{k_3}\ddot{x}_2 \tag{70}$$

Since $\bar{x}_1$ and $\ddot{x}_2$ are both equal to zero, $\ddot{x}_3$ is also equal to zero. Thus Eq. (69) is reduced to Kx = 0. Since K is positive definite, this yields x = 0. Therefore, all the assumptions of Theorem 3 are satisfied and we are now assured that x will go to zero.

The closed-loop system is simulated with the same parameter choice as before. The three displacements are shown in Fig. 5. Here again the stabilization is achieved since the three displacements vanish as time increases.

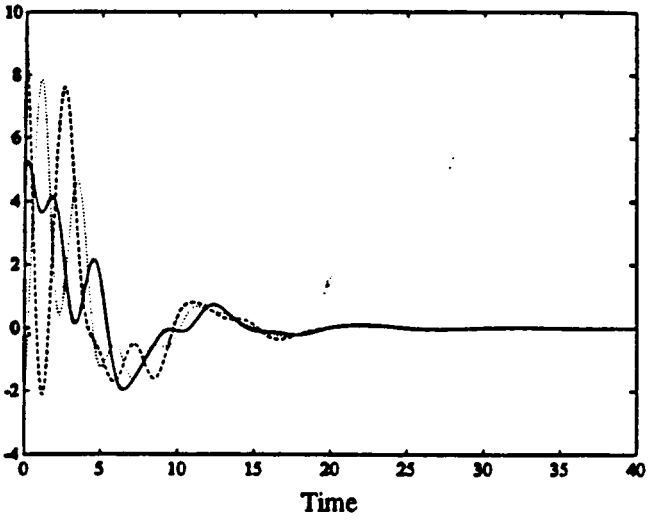

Figure 5 Displacements of x_1, x_2, and x_3

It is also possible to stabilize this system with a different distribution of forces. For instance, two controllers are applied to mass 2 and mass 3 or two controllers are applied to mass 1 and mass 3. The results are all similar to Fig. 5.

m=p=1

Here we design a control system with only one actuator. This actuator may be located on any of the three masses. Let us first apply a force on mass 1, i.e. the matrix B is

$$B = \begin{bmatrix} 1 \\ 0 \\ 0 \end{bmatrix} \tag{71}$$

Eq.(11) in Theorem 2 has the following obvious solution

$$\begin{aligned} \Lambda &= B^T \\ H_v &= \frac{1}{2} \\ B' &= \lambda \\ M_a &= \frac{1}{\lambda} \end{aligned} \tag{72}$$

where λ is an arbitrary strictly positive real number. The state x_a is calculated by integrating the differential equation

$$\ddot{x}_a = \ddot{x}_1 + \frac{1}{\lambda} u \tag{73}$$

The output of the system is $y = \frac{1}{\lambda}\dot{x}_a$.

Here again a SPR controller is chosen to be constant. Its transfer matrix is of the form G(s) = k, where k is any strictly positive real number. With this choice x converges to zero.

It should be checked as before that $B^T \dot{\bar{x}} = 0$ and u=0 imply $\ddot{\bar{x}} = 0$. The procedure is unchanged and once again those assumptions yield K x = 0. Since K is assumed to be positive semi-definite, x must be equal to zero.

The simulation is run with the same choice of initial conditions. The constant λ is still equal to 0.5, and k is equal to 1. The three displacements go to zero as expected which can be seen in Fig. 6.

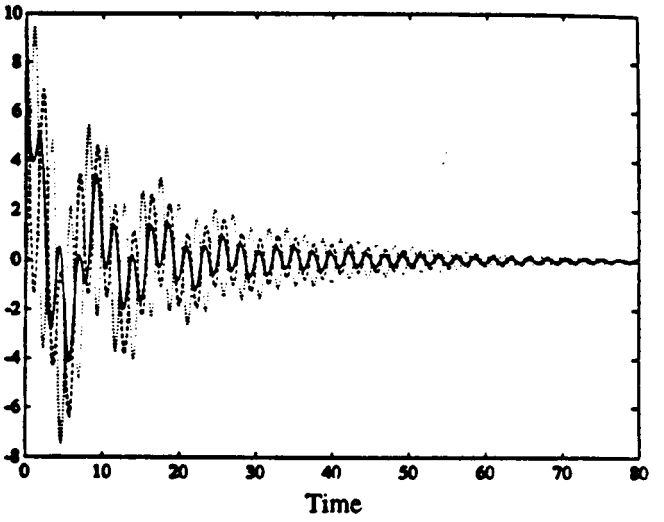

Figure 6 Displacements of x_1, x_2, and x_3

The force could be applied to mass 3. However, if we choose to apply the force on mass 2, the design cannot be completed. In this case,

$$B = \begin{bmatrix} 0 \\ 1 \\ 0 \end{bmatrix} \tag{73}$$

It can be checked that condition (i) of Theorem 3 is not satisfied. Thus no controller design can be implemented with the above choice.

To see the robust stability, let's study the example with m=n=p=3 again. The system is now perturbed to m_1=1.5, m_2=2, m_3=3, k_1=2, k_2=1.5, and k_3=3.5 while the controller is kept the same as before. The simulation is shown in Fig. 7 which clearly indicates robust stability.

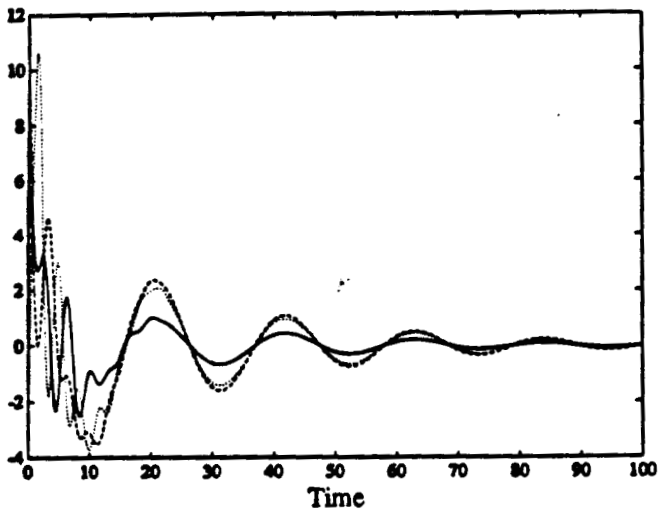

Figure 7 Displacements of x_1, x_2, and x_3

The second system consists of one spring and one mass. The system is described by

$$\begin{aligned} m\ddot{x} + kx &= u \\ y &= \ddot{x} \end{aligned} \tag{75}$$

If a simple integration of the output acceleration is used for the feedback control, it can be shown that

$$\lim_{t\to\infty} = \frac{d}{k}[\dot{x}(0) - c(0)] \tag{76}$$

where d is the feedback gain, $\dot{x}(0)$ is the true initial velocity, and c(0) is the estimated initial velocity. Since velocity is not measurable, c(0) is not equal to $\dot{x}(0)$. Therefore, asymptotic stability is not achieved.

However, if a virtual system is used by selecting

$$A = 1, H_v = \frac{1}{2}, B' = 1, M_a = 1 \tag{77}$$

The global system is robustly positive real. Using a simple constant feedback with 2d as the gain leads to the following closed-loop system

$$\begin{aligned} m\ddot{x} + kx &= u \\ \ddot{x}_a &= \ddot{x} + u \\ u &= -d\dot{x}_a \end{aligned} \tag{78}$$

It can be shown that

$$\begin{aligned} &\lim_{t\to\infty}[\int_0^t x\,dt - (\frac{m+1}{k})\dot{x}(0)] = 0 \\ &\lim_{t\to\infty} x(t) = 0 \end{aligned} \tag{79}$$

regardless of the initial velocity $\dot{x}(0)$. Therefore, the asymptotic stability of this design is independent of the initial velocity.

The performance of the controller can be obtained by optimization. The real part of the closed-loop eigenvalues can be minimized with respect to the feedback gain. For m=1 and k=1, the optimal feedback gain d is calculated to be d=0.52. Fig. 8 shows the response for the optimal feedback gain d=0.52, and Fig. 9 shows the response for the feedback gain d=2. It is clear that when d=0.52 the system performs better than the system with d=2. The robust performance is also demonstrated in Fig. 9 in which the mass and spring constants are perturbed to m=1.5 and k=1.2.

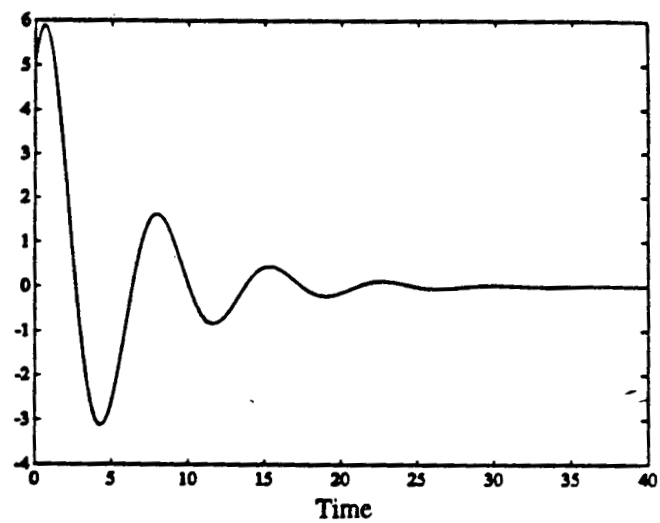

Figure 8 Displacement for d=0.52

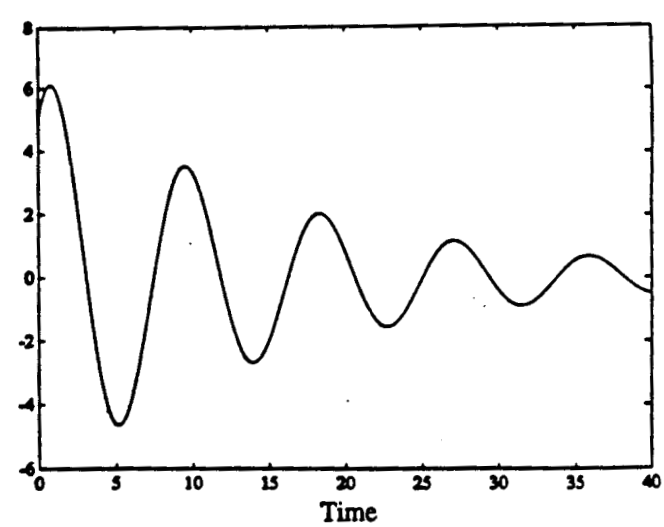

Figure 9 Displacement for d=2

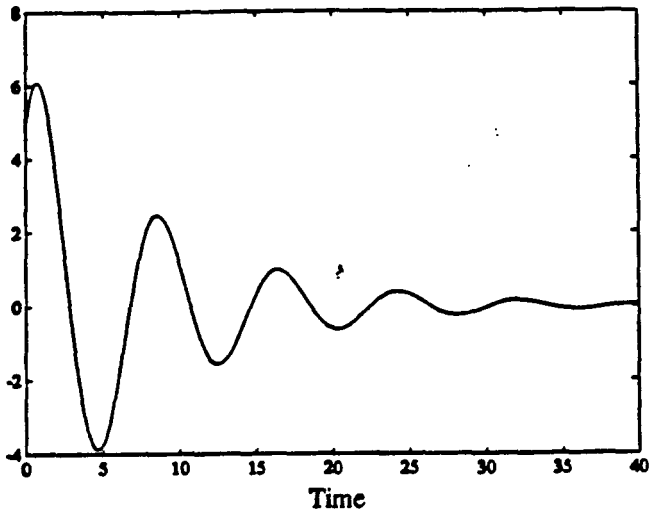

Figure 10 Displacement for m=1.5, k=1.2, and d=0.52

6. CONCLUSIONS

In this paper, a virtual system has been developed for second-order systems with only acceleration output. The combined system of the virtual system and the second-order system is positive real which allows infinite uncertainty in mass, spring constant, and damping coefficient. The states of the virtual system are not necessary the same as the states of the plant. The number of the virtual states can be made smaller than the number of the plant states. Furthermore, any strictly positive real controllers can be used to achieve the asymptotic stability of the closed-loop system. This design is particular of interest for practical applications since only acceleration measurement is required. Asymptotic stability can be achieved with infinite uncertainty in the system parameters and a large set of SPR controllers can be selected to optimize the performance. Two spring-mass systems have been used to demonstrate the virtual systems and controller designs. Extension to robust performance along this line of research is possible since one of the examples has been shown with some degree of robust performance.

REFERENCES

[1] R.J. Benhabib, R.P. Iwens, and R.L. Jackson, "Stability of Large Space Structure Control Systems Using Positivity Concepts," *J. of Guidance, Dynamics and Control*, Vol. 4, No. 5, Sept.-Oct. 1981.

[2] M. Takahashi and G.L. Slater, "Design of a Flutter Mode Controller Using Positive Real Feedback," *J. of Guidance, Dynamics and Control*, Vol. 9, No. 3, May-June 1986.

[3] M. D. McLaren and G. L. Slater, "Robust Multivariable Control of Large Space Structures Using Positivity," *J. of Guidance, Dynamics and Control*, Vol. 10, No. 4, July-August 1987.

[4] J-N. Juang and M. Phan, "Robust Controller Designs for Second-order Dynamic Systems: A Virtual Approach," *NASA Technical Memorandum TM-102666*, May 1990.

[5] J-N. Juang, S-C. Wu, M. Phan, and R.W. Longman, "Passive Dynamic Controllers for Nonlinear Mechanical Systems," *NASA Technical Memorandum 104047*, March 1991.

[6] K.A. Morris and J.N. Juang, "Robust Controller Design for Structures with Displacement Sensors," *Proceedings of the 30th Conference on Decision and Control*, December 1991.

[7] I. Bar-Kana, R. Fischl, and Paul Kalata, "Direct Position Plus Velocity Feedback Control of Large Flexible Space Structures," *IEEE Transactions on Automatic Control*, Vol. 36, No. 10, October 1991.

[8] D. Hill and P. Moylan, "The Stability of Nonlinear Dissipative Systems," *IEEE Transactions on Automatic Control*, October 1976.

[9] P.J. Moylan, "Implications of Passivity in a Class of Nonlinear Systems," *IEEE Transactions on Automatic Control*, Vol. ac-19, No. 4, August 1974.

[10] Q. Wang, J.L. Speyer, and H. Weiss, "System Characterization of Positive Real Conditions," *Proceedings of the 29th Conference on Decision and Control*, December 1990.

[11] C.-H. Chuang, O. Courouge, and J-N Juang, "Controller Designs for positive Real Second-Order Systems," *Proceedings of 1st International Motion and Vibration Control*, Sept. 1992.

AIAA-93-3867-CP

A PASSIVITY BASED CONTROLLER FOR FREE BASE MANIPULATORS

C. -H. Chuang* and Manoj Mittal**
School of Aerospace Engineering
Georgia Institute of Technology
Atlanta, Georgia

and

Jer-Nan Juang†
Spacecraft Dynamics Branch
NASA Langley Research Center
Hampton, Virginia

Abstract

A feedback linearization technique is used in conjunction with passivity concepts to design robust controllers for free base robots. It is assumed that bounded modeling uncertainties exist in the inertia matrix and the vector representing the coriolis, centripetal, and friction forces. Under these assumptions, the controller guarantees asymptotic tracking of the joint variables. A Lagrangian approach is used to develop a dynamic model for space robots. Closed-loop simulation results are illustrated for a simple case of a single link planar space manipulator with freely floating base.

Introduction

The dynamics of the space manipulators differs from that of the ground based manipulators since their base, the spacecraft, is free to move. The movement of the manipulator produces reaction forces and torques on the base. Therefore the resulting motion of the spacecraft has to be accounted for in the dynamic model for the manipulator. However, it is shown in reference [1] that a dynamic model for space robots developed by taking into account the motion of its base is similar in structure to dynamic models of fixed base manipulators. For instance, the inertia matrix in each case is symmetric and positive definite.

A few concepts have been proposed for joint trajectory control and inertial end tip motion control of space manipulators. Vafa and Dubowsky [2] developed an analytical tool for space manipulators, known as the virtual manipulator concept. The virtual manipulator is an idealized kinematic chain connecting its base, the virtual base, to any point on the real manipulator. This point can be chosen to be the manipulator's end effector, while the virtual base is located at the system center of mass, which is fixed in inertial space. As the real manipulator moves, the end of the virtual manipulator remains coincident with the selected point on the real manipulator. Additionally, it can be shown that the change in orientation in the virtual manipulator's joints is equal to the change in the orientation of the real manipulator's joints. While these features give the designer the ability to represent a free floating space manipulator by a simpler system whose base is fixed in inertial space, the associated transformation depends on knowing the system parameters exactly. Alexander and Cannon [3] showed that the end tip of the space robot can be controlled by solving the inverse dynamics that includes motion of the base. Their method assumes the mass of the spacecraft to be relatively large compared to that of the manipulator it carries, and also requires much computational effort to determine the control input. Note that, future systems are expected to have the manipulator and spacecraft masses of the same order. Umetani and Yoshida [4] proposed the generalized Jacobian matrix that relates the end tip velocities to the joint velocities by taking into account the motion of the base. The control method presented in the above reference is based on the concept of Resolved Motion Rate Control. However, only the kinematic problem was treated. Masutani et. al. [5] proposed a sensory feedback control scheme based on an artificial potential defined in the sensor coordinate frame. This scheme is based on proportional feedback of errors in the end tip position and orientation as well as feedback of joint angular velocities.

In this paper a robust control scheme based on feedback linearization and passivity concepts is proposed for space robots. A similar control scheme has been proposed earlier for fixed base robots [6]. The extension to space robots is in the spirit of the [1],

---

* Assistant Professor, AIAA Senior Member.

** Postdoctoral Fellow, AIAA Member.

† Prinicipal Scientist, AIAA Fellow.

where it was proposed that due to the striking similarity in the structure of the equations of motion of fixed and free base robots; almost any control scheme used for fixed base robots can be applied to free base robots. The control scheme uses inverse dynamics; however, it is robust in the face of bounded modeling uncertainties which might be due to imprecise modeling and/or intentional simplifications to the model based control law in order to reduce computational effort. The controller asymptotically tracks prescribed time varying joint angle trajectories whose acceleration is bounded in the L^2 space.

Dynamics of Space Manipulator System without Attitude Control of the Base

The development of the equations of motion for space robots presented here closely follows that given in [5]. A space manipulator system in the satellite orbit can be approximately considered to be floating in a non-gravitational environment. As shown in Figure 1, the manipulator and the base can be treated as a set of n+1 rigid bodies connected through n joints. The bodies are numbered from zero to n with the base being 0 and the end tip being n. Each joint is then numbered accordingly from one to n. The angular displacements of the joints can be represented by a joint vector,

$$q = [q_1\ q_2 \cdots q_n]^T \tag{1}$$

The mass and inertia tensor of the i^{th} body are denoted by m_i and I_i, and the inertia tensor is expressed in the base frame coordinates.

Kinematics

A coordinate frame fixed to the orbit of the satellite can be considered to be an inertial frame, denoted by Σ_I. In addition to Σ_I, another coordinate frame Σ_B is defined that is attached to the base with its origin located at the base center of mass. The attitude of the base itself is given by roll, pitch, and yaw angles. In the sequel, all vectors are expressed in the base fixed coordinate axes.

Let V_i and Ω_i be the linear and angular velocities with respect to the inertial frame, and ω_i be the angular velocity with respect to the base frame for the i^{th} link. Then for the i^{th} link

$$V_i = V_B + v_i + \Omega_B \times r_i \tag{3}$$

$$\Omega_i = \Omega_B + \omega_i \tag{4}$$

where r_i is the position vector of the i^{th} body with respect to the base center of mass, and $v_i = \dot{r}_i$. V_B and Ω_B are the linear and angular velocities of the base with respect to the inertial frame. v_i and ω_i for each link can be represented by the following forms

$$v_i = J_{Li}(q)\dot{q} \tag{5}$$

$$\omega_i = J_{Ai}(q)\dot{q} \tag{6}$$

where $J_{Li}(q)$ and $J_{Ai}(q) \in R^{3xn}$ are the Jacobian matrices for the i^{th} link.

The position of the system center of mass with respect to the base frame depends on the joint angles. Given below are two measures related to the system center of mass

$$m_c = \sum_{i=0}^{n} m_i \tag{7}$$

$$r_c(q) = \sum_{i=0}^{n} m_i r_i(q)/m_c \tag{8}$$

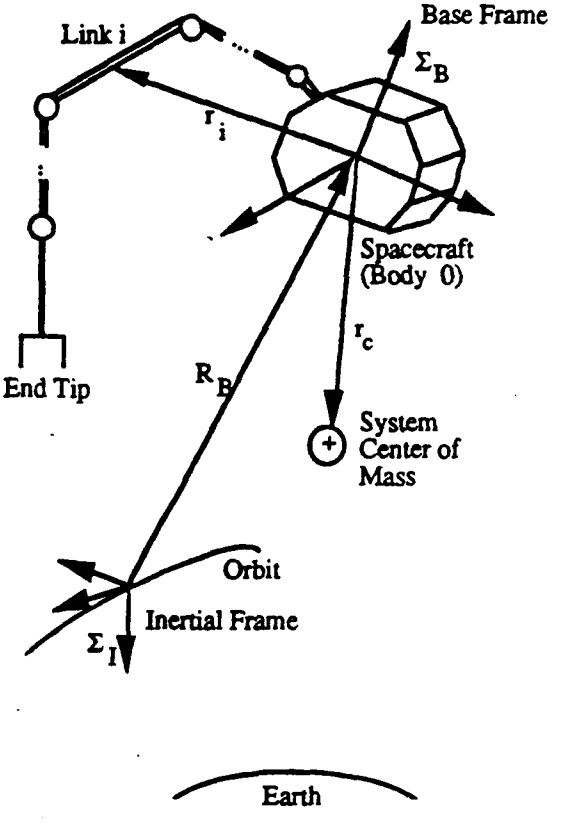

Figure 1. A Free Base Space Robot.

Dynamics

The total kinetic energy of the space robot can be written as

$$T = \frac{1}{2}\dot{q}^T D(q)\dot{q}, \quad D \in R^{n\times n} \tag{9}$$

where D is the inertia matrix of the system and is given by

$$D = H_q - \begin{bmatrix} H_{vq}^T & H_{\Omega q}^T \end{bmatrix} \begin{bmatrix} H_v & H_{v\Omega} \\ H_{v\Omega}^T & H_\Omega \end{bmatrix}^{-1} \begin{bmatrix} H_{vq} \\ H_{\Omega q} \end{bmatrix} \tag{10}$$

It can be shown that $D = D^T > 0$. H_q is the inertia matrix corresponding to the fixed base manipulator

$$H_q = \sum_{i=1}^{n} \left[m_i J_{Li}^T J_{Li} + J_{Ai}^T I_i J_{Ai} \right], \quad H_q \in R^{n\times n} \tag{11}$$

The second term on the right hand side of Equation (10) arises due to the fact that the base of the space robot is free. Since the working environment is non-gravitational and no actuators generating external forces are employed, the linear and angular momenta of the whole system are conserved. Since the inertial frame is fixed to the orbit, the whole system can be assumed to be stationary at the initial state. Thus the above two momenta are always zero for the whole system. Note that it is implicitly implied that the satellite is a non-spinning body. Using the assumption of zero initial momenta the individual components comprising the second term on the right hand side of Equation (10) can be written as

$$H_v = m_c I_{3\times 3}, \quad H_v \in R^{3\times 3} \tag{12}$$

$$H_\Omega = \sum_{i=0}^{n} I_i + \sum_{i=1}^{n} m_i [r_i\times]^T [r_i\times], \quad H_\Omega \in R^{3\times 3} \tag{13}$$

$$H_{v\Omega} = -m_c [r_c\times], \quad H_{v\Omega} \in R^{3\times 3} \tag{14}$$

$$H_{vq} = \sum_{i=1}^{n} m_i J_{Li}, \quad H_{vq} \in R^{3\times n} \tag{15}$$

$$H_{\Omega q} = \sum_{i=1}^{n} \left\{ I_i J_{Ai} + m_i [r_i\times] J_{Li} \right\}, \quad H_{\Omega q} \in R^{3\times n} \tag{16}$$

where for any vector

$$f = \begin{pmatrix} f_1 \\ f_2 \\ f_3 \end{pmatrix} \tag{17}$$

$$[f\times] \equiv \begin{pmatrix} 0 & -f_3 & f_2 \\ f_3 & 0 & -f_1 \\ -f_2 & f_1 & 0 \end{pmatrix} \tag{18}$$

and $I_{3\times 3}$ is the 3x3 identity matrix.

Since there is no potential energy in non-gravitational environment, the Lagrangian, Λ, is equal to the kinetic energy

$$\Lambda = T \tag{19}$$

So the system dynamics are given by

$$\frac{d}{dt}\left(\frac{\partial \Lambda}{\partial \dot{q}}\right) - \frac{\partial \Lambda}{\partial q} = \tau \tag{20}$$

where τ is an nx1 vector of input torques. Paralleling the development for fixed base robots in [7], the equations of motion for space robots can be written as,

$$D(q)\ddot{q} + h(q,\dot{q}) = \tau \tag{21}$$

where

$$h(q,\dot{q}) = C(q,\dot{q})\dot{q} \tag{22}$$

and the elements of the matrix C are given by

$$C_{Kj} = \frac{1}{2}\sum_{i=1}^{n} \left\{ \frac{\partial D_{Kj}}{\partial q_i} + \frac{\partial D_{Ki}}{\partial q_j} - \frac{\partial D_{ij}}{\partial q_k} \right\} \dot{q}_i \tag{23}$$

Base Motion

The conservation of linear and angular momenta yields expressions for the base translational and angular velocities

$$\begin{bmatrix} V_B \\ \Omega_B \end{bmatrix} = -\begin{bmatrix} H_v & H_{v\Omega} \\ H_{v\Omega}^T & H_\Omega \end{bmatrix}^{-1} \begin{bmatrix} H_{vq} \\ H_{\Omega q} \end{bmatrix} \dot{q} \tag{24}$$

Using the above expressions, the evolution of the base position and orientation with time can be determined as follows

$$\begin{bmatrix} \dot{x}_b \\ \dot{y}_b \\ \dot{z}_b \end{bmatrix} = \begin{bmatrix} c_\psi c_\theta & c_\psi s_\theta s_\phi - s_\psi c_\phi & c_\psi s_\theta c_\phi + s_\psi s_\phi \\ s_\psi c_\theta & s_\psi s_\theta s_\phi + c_\psi c_\phi & s_\psi s_\theta c_\phi - c_\psi s_\phi \\ -s_\theta & c_\theta s_\phi & c_\theta c_\phi \end{bmatrix} V_B \tag{25}$$

$$\begin{bmatrix} \dot{\phi} \\ \dot{\theta} \\ \dot{\psi} \end{bmatrix} = \begin{bmatrix} 1 & s_\phi \tan(\theta) & c_\phi \tan(\theta) \\ 0 & c_\phi & -s_\phi \\ 0 & s_\phi \sec(\theta) & c_\phi \sec(\theta) \end{bmatrix} \Omega_B \tag{26}$$

where

$$c_{(\cdot)} \equiv \cos(\cdot), \; s_{(\cdot)} \equiv \sin(\cdot) \tag{27}$$

Control System Design

Feedback Linearization

Assuming that the dynamics of the space robot are described by Equation (21), where D and h are completely known, the feedback linearization or inverse dynamics technique [7] can be used to design controllers for tracking prescribed command trajectories for the joint angles. This can be accomplished by letting

$$\tau = Du + h \tag{28}$$

where u is the pseudo-control, i.e., it is the control input to the linearized system. With the control law given by Equation (28), the closed-loop system becomes

$$\begin{Bmatrix} \dot{q} \\ \ddot{q} \end{Bmatrix} = A \begin{Bmatrix} q \\ \dot{q} \end{Bmatrix} + Bu \tag{29}$$

where

$$A = \begin{bmatrix} 0 & I \\ 0 & 0 \end{bmatrix}, B = \begin{bmatrix} 0 \\ I \end{bmatrix} \tag{30}$$

A simple PD (Proportional-Derivative) type of control law is chosen for the feedback linearized system

$$u = \ddot{q}_d + K_2(\dot{q}_d - \dot{q}) + K_1(q_d - q) \tag{31}$$

where K_1 and K_2 are proportional and derivative gain matrices, respectively. These matrices are usually chosen to be diagonal in order to achieve decoupled response among the joint angles. Substituting for u from Equation (31) into Equation (29), one obtains

$$\dot{e} = A_c e \tag{32}$$

where $e = [e_1^T \; e_2^T]^T, e_1 = q_d - q, e_2 = \dot{q}_d - \dot{q}$ and $A_c = A - BK$. If $K_1 > 0$ and $K_2 > 0$, the error dynamics as given by Equation (32) are asymptotically stable. The freedom in selecting the gain matrices can be utilized to meet performance specifications for the closed-loop system.

The preceding discussion assumes availability of perfect knowledge about the system dynamics. However, in practice, D and h are usually imprecisely known due to modeling inaccuracies. Furthermore, D and h may be too complex to be used for real-time control implementation. In the following sub-section, a control law that is robust for bounded uncertainties in D and h is given. The control law results in closed-loop asymptotic tracking.

Robust Feedback Linearization Using Passivity

The development in this section follows that given in [6] very closely. In the presence of modeling uncertainties, the control law is given as

$$\tau = D_c u + h_c \tag{33}$$

where D_c and h_c are computed versions of D and h respectively. Substituting for τ and u from Equations (33) and (31) into Equation (21) it can be shown that the closed-loop system dynamics are given by

$$\dot{e} = A_c e + Bv \tag{34}$$

where

$$v = \Delta u + \delta \tag{35}$$

and

$$\Delta = (I - D^{-1}D_c), \; \delta = D^{-1}(h - h_c) \tag{36}$$

The first step in the design proposed in [6] is to choose the gain matrix $K = [K_1 \; K_2]$ and an output matrix F such that the linear system given by

$$\begin{aligned} \dot{e} &= A_c e + Bv \\ y &= Fe \end{aligned} \tag{37}$$

is SPR (Strictly Positive Real) [8]. This can be achieved as follows.

Theorem 1 [6]. Let K_1 and K_2 be such that

$$\begin{aligned} K_1 &= \text{diag}[k_{1i}]; \; k_{1i} > 0, i = 1,\ldots,n \\ K_2 &= \text{diag}[k_{2i}]; \; k_{2i} > 0, i = 1,\ldots,n \\ (k_{2i})^2 &> k_{1i}, \qquad i = 1,\ldots,n \end{aligned} \tag{38}$$

then if F = K, the system described by Equation (37) is SPR.

The proof is omitted here, the interested reader is referred to [6]. Note that the conditions of the theorem given in Equations (38) are extremely easy to satisfy.

With the linear system (37) being SPR, the passivity theorem [9] can be used to design asymptotically stable controllers as shown in the following theorem. The theorem is very similar to that given in [6], with the only difference being in the way in which the uncertainty bound on the h vector is characterized.

Theorem 2. Let the following two inequalities hold

$$D < \frac{1}{r} I \quad (r > 0) \tag{39}$$

$$\left\| D^{-1}(h - h_c) \right\|_T \le c\|u\|_T + d \quad \forall T > 0 \quad (c \ge 0, d \ge 0) \tag{40}$$

Furthermore, let $\ddot{q}_d \in L^2$. Then if $D_c = aI$ where

$$a > \frac{c+1}{r} \tag{41}$$

the closed-loop system is asymptotically stable.

Proof. The closed-loop system as given by Equation (34) can be represented in block diagram form as shown in Figure 2. It is first shown that the nonlinear block in the feedback path is passive [9].

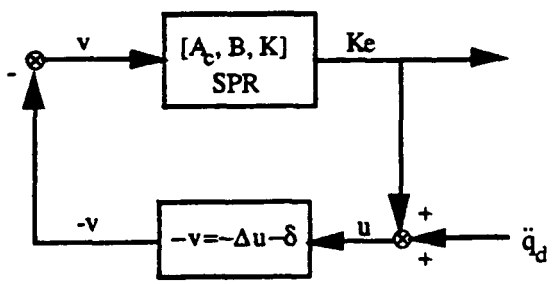

Figure 2. Robust Feedback Linearization Using Passivity Theorem.

Consider

$$\begin{aligned} I &= \int_0^T -u^T v\,dt \quad (T > 0) \\ &= \int_0^T -u^T(\Delta u + \delta)\,dt \\ &= \left(-\int_0^T u^T \Delta u\,dt \right) + \left(-\int_0^T u^T \delta\,dt \right) \end{aligned} \tag{42}$$

Let the first and second integrals on the right hand side be denoted by I_1 and I_2 respectively. Then

$$I_1 = \int_0^T u^T (aD^{-1} - I) u\,dt \tag{43}$$

Noting that

$$D < \frac{1}{r} I \;\Rightarrow\; aD^{-1} - I > (ar - 1) I \tag{44}$$

one can obtain

$$I_1 \ge (ar - 1)\|u\|_T^2 \tag{45}$$

On the other hand,

$$\begin{aligned} -I_2 &= \int_0^T u^T D^{-1}(h - h_c)\,dt \\ &\le \|u\|_T \left\| D^{-1}(h - h_c) \right\|_T \quad \text{(Hölder's Inequality)} \\ &\le \|u\|_T [c\|u\|_T + d] \end{aligned} \tag{46}$$

Hence

$$I \ge (ar - c - 1)\|u\|_T^2 - d\|u\|_T = f\left(\|u\|_T\right) \tag{47}$$

It can be shown that if (ar - c - 1) > 0, then

$$f\left(\|u\|_T\right) \ge -\frac{d^2}{4(ar - c - 1)} \quad \forall \|u\|_T \ge 0 \tag{48}$$

Hence

$$\int_0^T -u^T v\,dt \ge -\frac{d^2}{4(ar - c - 1)} \quad \forall T > 0 \tag{49}$$

Thus a sufficient condition for the nonlinear block to be passive is that a > (c + 1)/r.

Additionally, the transfer function of the feedforward block $[A_C, B, K]$ is proper and has no poles on the imaginary axis. Hence it has finite gain [10]. Since $\ddot{q}_d \in L^2$, then using the passivity theorem [9], one can conclude that the signals u, Ke, and v are bounded. Moreover, since the feedforward block is SPR, $Ke(t) = K_1 e_1(t) + K_2 e_2(t)$ goes to zero asymptotically. This in turn implies that $e_1(t)$ and $e_2(t)$ individually approach zero asymptotically [8].

The first condition of the theorem, given by Equation (39), is easy to satisfy since D is upper bounded. However, the second condition, given by Equation (40), might not be easy to verify in a straightforward manner in all applications.

Simulation Results

As an example, results are illustrated for a single link space robot shown in Figure 3. Equation (21) describes the dynamics of this one degree of freedom system. The system inertia, computed using Equation (10), turns out to be

$$D(q_1) = m'P_1^2 + I_1 - \frac{1}{d}[m'P_1(P_o c_1 + P_1) + I_1]^2 \quad (50)$$

where

$$d = m'(P_o^2 + P_1^2 + 2P_o P_1 c_1) + I_o + I_1 \quad (51)$$

and $m' = m_0 m_1 / (m_0 + m_1)$. Using Equations (22) and (23), h is determined to be

$$h(q_1, \dot{q}_1) = \frac{m'P_o P_1 s_1}{d^2}[m'P_o(P_o + P_1 c_1) + I_o] \cdot [m'P_1(P_o c_1 + P_1) + I_1]\dot{q}_1^2 \quad (52)$$

In Equations (50) through (52), $c_1 \equiv \cos(q_1), s_1 \equiv \sin(q_1)$.

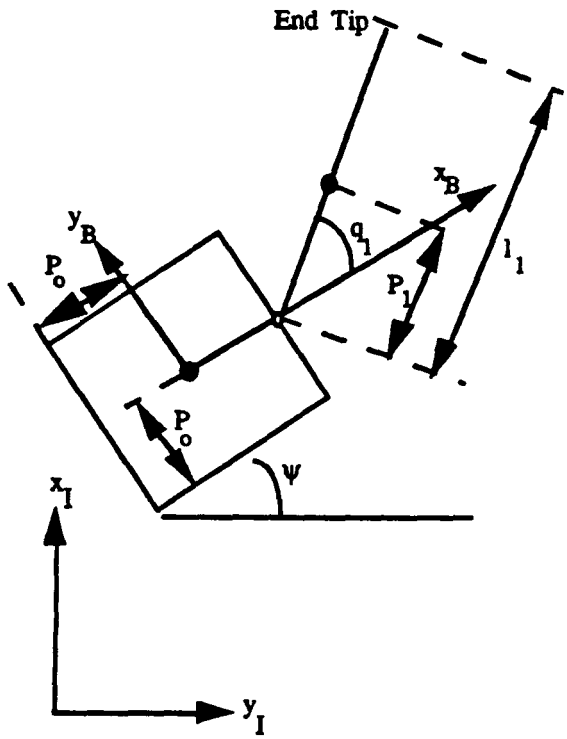

Figure 3. A Single Link Planar Space Robot.

It can be seen easily that as $m_0 \to \infty$, and $I_0 \to \infty$,

$$D \to m_1 P_1^2 + I_1, \; h \to 0 \quad (53)$$

which represents the case of a fixed base manipulator. Equation (25) is used to determine the evolution of the base position with time

$$\dot{x}_b = \frac{m'}{m_0}\left[P_1 s_{\psi 1} - \frac{1}{d}\{m'P_1(P_o c_1 + P_1) + I_1\} \cdot (P_1 s_{\psi 1} + P_o s_\psi)\right]\dot{q}_1$$

$$\dot{y}_b = \frac{m'}{m_0}\left[-P_1 c_{\psi 1} + \frac{1}{d}\{m'P_1(P_o c_1 + P_1) + I_1\} \cdot (P_1 c_{\psi 1} + P_o c_\psi)\right]\dot{q}_1 \quad (54)$$

where

$$s_{\psi 1} = \sin(\psi + q_1), \; c_{\psi 1} = \cos(\psi + q_1) \quad (55)$$

Finally, the base attitude dynamics is obtained using Equation (26)

$$\dot{\psi} = -\frac{1}{d}[m'P_1(P_o c_1 + P_1) + I_1]\dot{q}_1 \quad (56)$$

Next, a feedback controller is designed for the space robot using the results of Theorems 1 and 2. Closed-loop results are generated for a step command of 1 radian to the joint angle. Note that in general, for end tip motion control in the inertial space, the inverse kinematics problem needs to be solved to generate a command trajectory for the joint angle. Table 1 lists physical parameters of the example robot used in simulation. The base and link masses are of the same order of magnitude.

Table 1. Physical Parameters of Example Robot.

Body	p (meter)	l (meter)	m (kg)	I (kg.m^2)
0 (Base)	3.0	-	5.0	30.0
1 (Link)	3.0	6.0	1.0	3.0

The feedback gains are chosen to be $k_1 = 0.4$ and $k_2 = 1.0$. This choice of gains satisfies Equations (38) and in case of no modeling uncertainty, yields a closed-loop response without any overshoot. The fact that the system center of mass should remain stationary in inertial space is used to monitor numerical accuracy of integration. Simulation results are shown for the case in which there is no modeling uncertainty, and for two other cases that involve differing degrees of uncertainty. It is assumed that Equations (21) and (50) through (52) represent the true robot; the uncertainty is introduced in computing D and h. An upper bound for the system inertia, needed for condition (39) of Theorem 2, is given for this particular case by

$$\frac{1}{r} = m'P_1^2 + I_1 \quad (57)$$

a in Theorem 2 is assumed to be 1.1/r for both cases involving uncertainty. The choice of h_c however, is different for the two cases. In the first case, the

following simplification to h is used for computing the closed-loop control

$$h_c = m\dot{P}_o P_1 s_1 \dot{q}_1 \tag{58}$$

The second case corresponds to an even greater simplification to h

$$h_c = m\dot{P}_o P_1 \dot{q}_1 \tag{59}$$

Figures 4 through 7 show closed-loop results for the nominal case and for the first case involving uncertainty. c = 0.01 was chosen to satisfy condition (41) of Theorem 2. d was chosen to be 2.5. Figure 4 shows that asymptotic tracking in the joint angle is

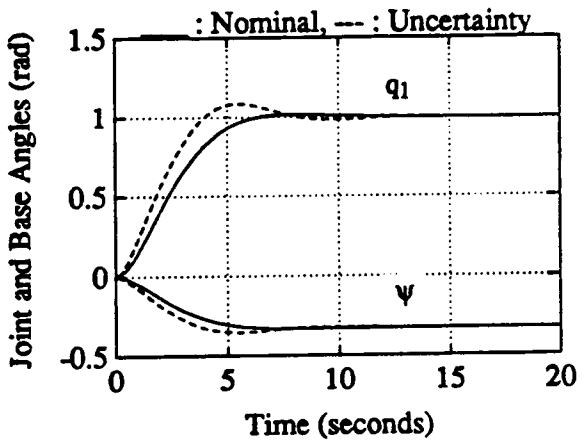

Figure 4. Joint and Base Angle Responses for the Nominal Case and the First Case Involving Uncertainty.

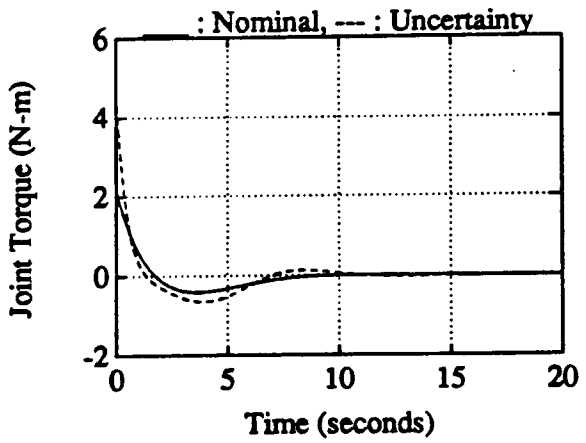

Figure 5. Joint Torque Input for the Nominal Case and the First Case Involving Uncertainty.

achieved in the face of uncertainty. This is associated with a slight performance degradation in the joint angle response in the sense that it has an overshoot. Figure 5 shows that higher magnitudes of joint torque are required for the case involving uncertainty. Figures 4 and 6 show that the base moves in reaction to link motion; this is due to the conservation of linear and angular momentum as discussed previously. However, the joint angle still achieves the right commanded value. Figure 7 shows that the choice of c and d used in this case satisfies condition (40) of Theorem 2.

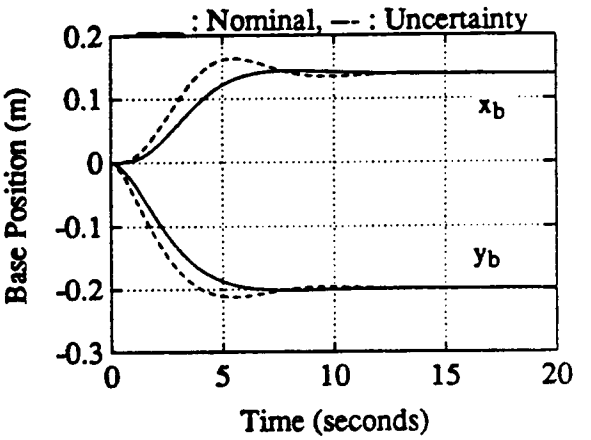

Figure 6. Motion of the Base Center of Mass for the Nominal Case and the First Case Involving Uncertainty.

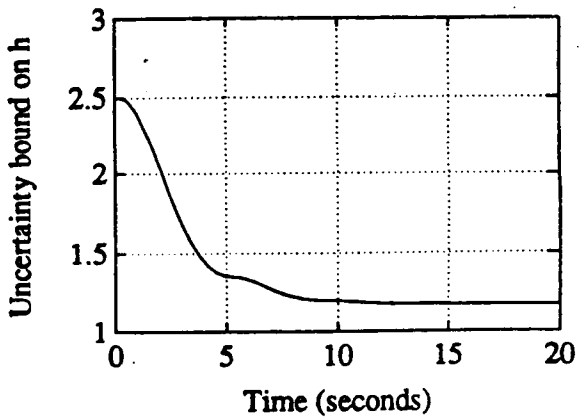

Figure 7. The Quantity $c\|u\|_T + d - \|D^{-1}(h - h_c)\|_T$ for the First Case Involving Uncertainty.

Figures 8 through 11 show closed-loop results for the nominal case and the second case involving uncertainty. For the second case, c and d are chosen to

be c = 0.01 and d = 5.0. Trends similar to the previous case are noticed here also. However, since the extent of uncertainty is greater, there is more deviation in the responses as compared to the previous case. This is observed in Figures 8 through 10. Figure 11 confirms that the choice of c and d satisfies the requirements of Theorem 2.

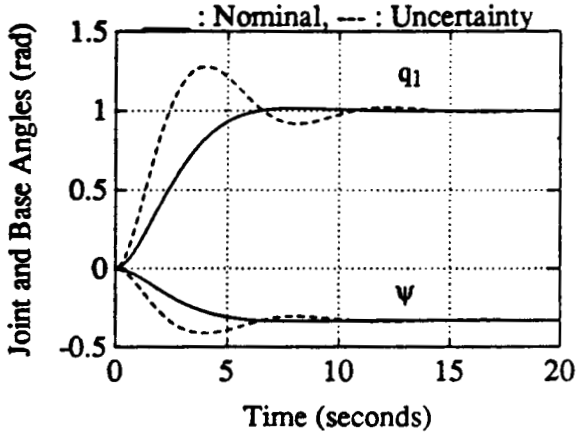

Figure 8. Joint and Base Angle Responses for the Nominal Case and the Second Case Involving Uncertainty.

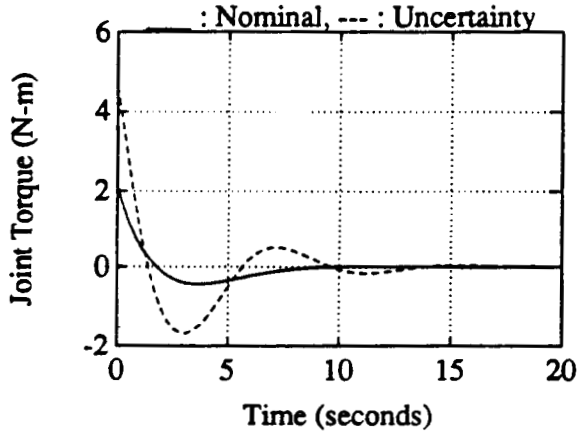

Figure 9. Joint Torque Input for the Nominal Case and the Second Case Involving Uncertainty.

Conclusions

A control method based on feedback linearization and passivity concepts that was proposed earlier for fixed base robots is modified and extended to the case of free base robots. The control law results in

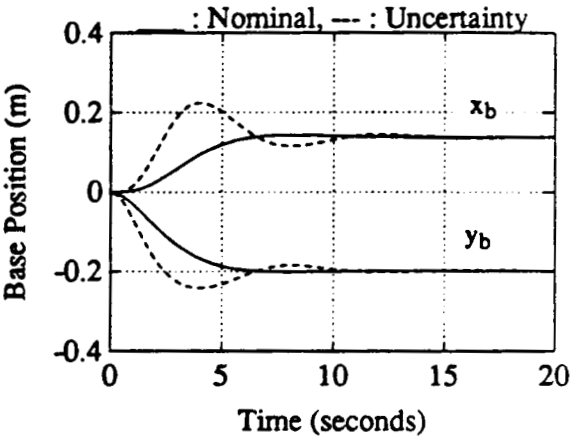

Figure 10. Motion of the Base Center of Mass for the Nominal Case and the Second Case Involving Uncertainty.

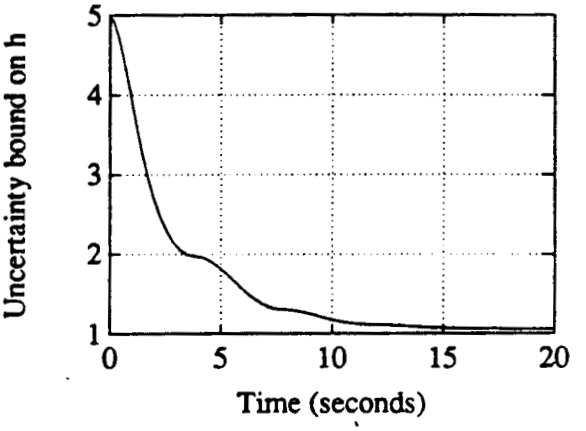

Figure 11. The Quantity $c\|u\|_T + d - \|D^{-1}(h - h_c)\|_T$ for the Second Case Involving Uncertainty.

asymptotic joint angle tracking in the face of bounded uncertainties. For the first time, closed-loop simulation results are presented using this control method. For the simple example illustrated in the paper, the control method shows promising results.

References

[1]. E. Papadopoulos and S. Dubowsky, "On the Nature of Control Algorithms for Space Manipulators," Proceedings of the 1990 IEEE International Conference on Robotics and Automation, Cincinnati, Ohio, pp. 1102-1108.

[2]. Z. Vafa and S. Dubowsky, "The Kinematics and Dynamics of Space Manipulators: The Virtual Manipulator Approach," The International Journal of Robotics Research, Raleigh, 9(4), August 1990.

[3]. H. L. Alexander and R.H. Cannon, "Experiments on the Control of a Satellite Manipulator," Proceedings of the 1987 American Control Conference, Minneapolis, Minnesota.

[4]. Y. Umetani and K. Yoshida, "Continuous Path Control of Space Manipulators Mounted on OMV," Acta Astronautica, 15(12), 1987, pp. 981- 986.

[5]. Y. Masutani, F. Miyazaki, and S. Arimoto, "Sensory Feedback Control For Space Manipulators," Proceedings of the 1989 IEEE International Conference on Robotics and Automation, Scottsdale, Arizona.

[6]. C. Abdallah and R. Jordan, "A Positive-Real Design for Robotic Manipulators," Proceedings of the 1990 American Control Conference, San Diego, California, pp. 991-992.

[7]. M. W. Spong and M. Vidyasagar, Robot Dynamics and Control, John Wiley, New York, 1989.

[8]. J-J. E. Slotine and W. Li, Applied Nonlinear Control, Prentice Hall, New Jersey, 1991, pp. 127, 399.

[9]. C. A. Desoer and M. Vidyasagar, Feedback Systems: Input-Output Properties, Academic Press, New York, 1975, pp. 173-186.

[10]. J. C. Doyle, B. A. Francis, and A. R. Tannenbaum, Feedback Control Theory, Macmillan, New York, 1992, pp. 16.

NONLINEAR CONTROL OF SPACE MANIPULATORS WITH MODEL UNCERTAINTY

Manoj Mittal* and C. -H. Chuang†
School of Aerospace Engineering
Georgia Institute of Technology
Atlanta, Georgia 30332-0150

and

Jer-Nan Juang‡
Spacecraft Dynamics Branch
NASA Langley Research Center
Hampton, Virginia

Abstract

For robotic manipulators, nonlinear control using feedback linearization or inverse dynamics yields good results in the absence of modeling uncertainty. However, modeling uncertainties such as unknown joint friction coefficients can give rise to undesirable characteristics when these control systems are implemented. In this work, it is shown how passivity concepts can be used to supplement the feedback linearization control design technique, in order to make it robust with respect to bounded uncertain effects. Results are obtained for space manipulators with freely floating base; however, they are applicable to fixed base manipulators as well. The controller guarantees asymptotic tracking of the joint states. Closed-loop simulation results are illustrated for a planar single link space manipulator.

1. Introduction

The dynamics of space manipulators differs from that of fixed base manipulators since their base is free to move. The base could be either a spacecraft or a satellite. The movement of manipulator arms produces reaction forces and torques on the base. Therefore the resulting motion of the base has to be accounted for in the dynamic modeling of the manipulator. However, Papadopoulos and Dubowsky[1] showed that a dynamic model for space manipulators with a free base is similar in structure to the dynamic model for fixed base manipulators. An obvious similarity is that the inertia matrix in each case is symmetric and positive definite. In fact, the dynamic model for fixed base manipulators can be viewed as a subset of the model for space manipulators. In the past, a great deal of attention has been paid by researchers in the area of dynamic modeling of space manipulators. Some interesting notions have emerged from modeling studies, of significant importance among which is the idea of virtual manipulators[2]. On the other hand, little effort has been made in the area of robust tracking control law synthesis for space manipulators. A few concepts have been proposed for joint trajectory control and inertial end tip motion control of space manipulators. Alexander and Cannon[3] showed that the end tip of a space robot can be controlled by solving the inverse dynamics that includes motion of the base. Their method assumes the mass of the spacecraft to be relatively large compared to that of the manipulator it carries, and also requires much computational effort to determine the control input. Note that some future space systems are expected to have the manipulator and spacecraft masses of the same order. Yoshida and Umetani[4] proposed the generalized Jacobian matrix that relates the end tip velocities to the joint velocities by taking into account the motion of the base. However, robustness of the control scheme with respect to modeling uncertainties was not addressed.

A nonlinear controller based on feedback linearization and passivity concepts was developed by Chuang, Mittal, and Juang[5]. The feedback linearization technique for nonlinear control system design has been generally accepted to yield good results. However, these type of controllers require full inversion of the nonlinear system model in real-time. This computational imposition can restrict and limit the applicability of the technique. In Ref. 5, it was shown that if simplifications to the nonlinear model are made in a manner such that the passivity of the closed-loop system is preserved in a certain sense, the feedback linearization technique retains it's asymptotic stabilization properties.

In this paper, a nonlinear dynamic model for space manipulators with uncontrolled base is first derived.

---

* Postdoctoral Fellow, AIAA Member.

† Assistant Professor, AIAA Senior Member.

‡ Principal Scientist, AIAA Fellow.

The development of the expressions for linear and angular momenta of the system closely follows that given in Ref. 6; however, the form of the final equations of motion is different. It is then shown how passivity concepts can be used in conjunction with the feedback linearization technique to design robust nonlinear controllers for space manipulators. The proposed control scheme can be used for fixed base manipulators also. The control scheme uses inverse dynamics; however, it is robust in the face of bounded modeling uncertainties which might arise due to a number of factors including improper friction modeling. The controller asymptotically tracks prescribed time varying joint angle trajectories whose acceleration is bounded in the L^2 space.

2. Nonlinear Dynamic Model of the Space Manipulator System

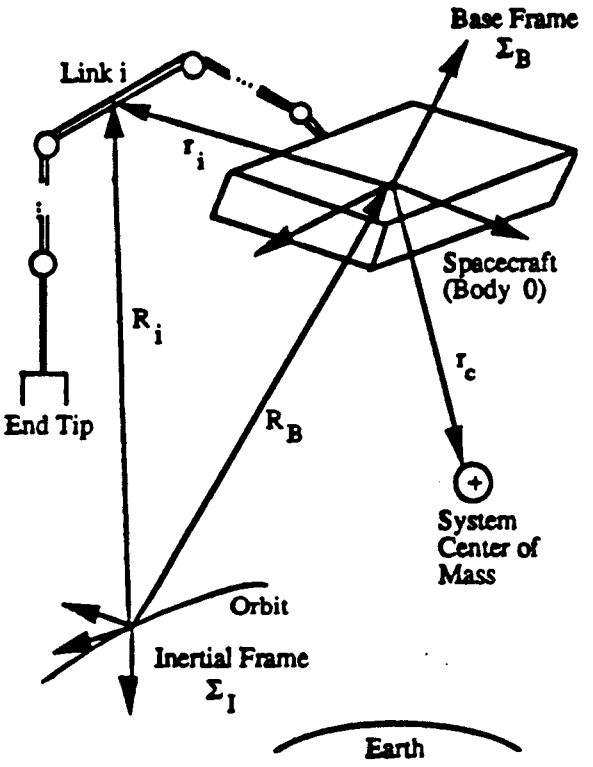

Fig. 1. A Space Robot.

The development of a nonlinear dynamic model for a space manipulator system whose base is uncontrolled is discussed in this Section. A space manipulator system in a satellite orbit can be approximately considered to be floating in a non-gravitational environment. As shown in Figure 1, the manipulator and the base can be treated as a set of n+1 rigid bodies connected through n joints. The bodies are numbered from zero to n with the base being 0 and the end tip being n. Each joint is then numbered accordingly from one to n. The angular displacements of the joints can be represented by a joint vector,

$$q = [q_1\ q_2 \cdots q_n]^T \tag{1}$$

The mass and inertia tensor of the i^{th} body are denoted by m_i and I_i; and the inertia tensor is expressed in terms of the base frame coordinates.

2.1 Kinematics

A coordinate frame fixed to the orbit of the satellite can be considered to be an inertial frame, denoted by Σ_I. In addition to Σ_I, another coordinate frame Σ_B is defined that is attached to the base with its origin located at the base center of mass. The attitude of the base itself is given by roll, pitch, and yaw angles. In the sequel, all vectors are expressed in the base fixed coordinate axes.

Let R_i and r_i be the position vectors of the center of mass of the i^{th} link with respect to frames Σ_I and Σ_B, respectively. Then

$$R_i = R_B + r_i \tag{2}$$

where R_B is the position vector from the origin of the frame Σ_I to the base center of mass. Let V_i and Ω_i be the linear and angular velocities of the center of mass of the i^{th} link with respect to frame Σ_I and v_i and ω_i be the linear and angular velocities of the same point with respect to frame Σ_B. Then V_i and Ω_i can be written as

$$V_i = V_B + v_i + \Omega_B \times r_i \tag{3}$$

$$\Omega_i = \Omega_B + \omega_i \tag{4}$$

V_B and Ω_B are the linear and angular velocities of the base center of mass with respect to frame Σ_I. Note that for any space manipulator, v_i and ω_i for each link can be represented by the following forms

$$v_i = J_{Li}(q)\dot{q} \tag{5}$$

$$\omega_i = J_{Ai}(q)\dot{q} \tag{6}$$

where $J_{Li}(q)$ and $J_{Ai}(q) \in R^{3xn}$ are the Jacobian matrices for the i^{th} link.

The position of the system center of mass with respect to the base frame depends on the joint angles. Given below are two measures related to the system center of mass.

$$m_c = \sum_{i=0}^{n} m_i \tag{7}$$

$$r_c(q)=\frac{\sum_{i=0}^{n} m_i r_i(q)}{m_c} \tag{8}$$

2.2 Linear and Angular Momenta

The linear momentum P and the angular momentum L of the whole system are defined as follows

$$P=\sum_{i=0}^{n} m_i V_i \tag{9}$$

$$L=\sum_{i=0}^{n}\left[I_i\Omega_i + m_i R_i \times V_i\right] \tag{10}$$

Substituting Equations (2) through (8) into Equations (9) and (10) yields

$$P = H_v V_B + H_{v\Omega}\Omega_B + H_{vq}\dot{q} \tag{11}$$

$$L = H_{v\Omega}^T V_B + H_\Omega \Omega_B + H_{\Omega q}\dot{q} + R_B \times P \tag{12}$$

where

$$H_v = m_c I_{3\times 3},\ H_v \in R^{3\times 3} \tag{13}$$

$$H_{v\Omega} = -m_c[r_c\times],\ H_{v\Omega}\in R^{3\times 3} \tag{14}$$

$$H_{vq} = \sum_{i=1}^{n} m_i J_{Li},\quad H_{vq}\in R^{3\times n} \tag{15}$$

$$H_\Omega = \sum_{i=0}^{n} I_i + \sum_{i=1}^{n} m_i[r_i\times]^T[r_i\times],\ H_\Omega \in R^{3\times 3} \tag{16}$$

$$H_{\Omega q} = \sum_{i=1}^{n}\left\{I_i J_{Ai} + m_i[r_i\times]J_{Li}\right\},\quad H_{\Omega q}\in R^{3\times n} \tag{17}$$

For any vector $f=[f_1\ f_2\ f_3]^T$, $[f\times]$ is defined as

$$[f\times]\equiv\begin{bmatrix} 0 & -f_3 & f_2 \\ f_3 & 0 & -f_1 \\ -f_2 & f_1 & 0\end{bmatrix}.$$

Since the working environment is non-gravitational and no actuators generating external forces are employed, the linear and angular momenta of the whole system are conserved. Since the inertial frame is fixed to the orbit, the entire system can be assumed to be stationary with respect to the inertial frame at the initial state. Thus the above two momenta are always zero for the system. Note that it is implicitly implied that the satellite is a non-spinning body. By using the fact that the linear and angular momenta are zero, Equations (11) and (12) result in

$$V_B = -H_v^{-1}\left[H_{v\Omega}\Omega_B + H_{vq}\dot{q}\right] \tag{18}$$

$$\Omega_B = -\left[H_\Omega - H_{v\Omega}^T H_v^{-1} H_{v\Omega}\right]^{-1}\cdot \left[H_{\Omega q} - H_{v\Omega}^T H_v^{-1} H_{vq}\right]\dot{q} \tag{19}$$

2.3 Manipulator Dynamics

The total kinetic energy of the space robot can be written as

$$T=\frac{1}{2}\sum_{i=0}^{n}\left(m_i V_i^T V_i + \Omega_i^T I_i \Omega_i\right) \tag{20}$$

Using Equations (3) through (8) and (13) through (17) the kinetic energy can be expressed as

$$T=\frac{1}{2}\begin{bmatrix} V_B^T & \Omega_B^T & \dot{q}^T\end{bmatrix}\begin{bmatrix} H_v & H_{v\Omega} & H_{vq} \\ H_{v\Omega}^T & H_\Omega & H_{\Omega q} \\ H_{vq}^T & H_{\Omega q}^T & H_q\end{bmatrix}\begin{bmatrix} V_B \\ \Omega_B \\ \dot{q}\end{bmatrix} \tag{21}$$

where H_q is the inertia matrix corresponding to the fixed base manipulator

$$H_q = \sum_{i=1}^{n}\left[m_i J_{Li}^T J_{Li} + J_{Ai}^T I_i J_{Ai}\right],\quad H_q\in R^{n\times n} \tag{22}$$

Equation (21) for the system kinetic energy can be simplified as follows. Substituting for V_B from Equation (18) leads to

$$T=\frac{1}{2}\Omega_B^T M \Omega_B + \Omega_B^T Z\dot{q} + \frac{1}{2}\dot{q}^T W\dot{q} \tag{23}$$

where

$$M = H_\Omega - H_{v\Omega}^T H_v^{-1} H_{v\Omega},\ M\in R^{3\times 3} \tag{24}$$

$$Z = H_{\Omega q} - H_{v\Omega}^T H_v^{-1} H_{vq},\ Z\in R^{3\times n} \tag{25}$$

$$W = H_q - H_{vq}^T H_v^{-1} H_{vq},\ W\in R^{n\times n} \tag{26}$$

Further, substituting for Ω_B from Equation (19), one obtains an expression for the system kinetic energy solely in terms of the joint variables.

$$T=\frac{1}{2}\dot{q}^T D(q)\dot{q},\quad D\in R^{n\times n} \tag{27}$$

where D is the inertia matrix of the system and is given by

$$D = W - Z^T M^{-1} Z \tag{28}$$

It can be shown that $D = D^T > 0$. It is interesting to note that the system inertia matrix obtained in Reference [1] is of the same form as above. However,

the expressions for W, M, and Z matrices are different. This is because a different approach, viz., the concept of barycenters, is used in the model derivation of Reference [1]. It is also noteworthy that the inertia matrix obtained above requires only a 3 x 3 matrix inversion, while that obtained by Masutani, Miyazaki, and Arimoto[6] requires a 6 x 6 matrix inversion.

Since there is no potential energy in non-gravitational environment, the Lagrangian Λ, is equal to the kinetic energy

$$\Lambda = T \tag{29}$$

So the system dynamics is given by

$$\frac{d}{dt}\left(\frac{\partial T}{\partial \dot{q}}\right) - \frac{\partial T}{\partial q} = \tau \tag{30}$$

where τ is the n x 1 vector of joint torques. The equation of motion for space manipulators is then obtained by using Equation (30).

$$D(q)\ddot{q} + h(q,\dot{q}) = \tau \tag{31}$$

where

$$h(q,\dot{q}) = C(q,\dot{q})\dot{q} + \tau_f \tag{32}$$

Paralleling the development for fixed base robots given by Spong and Vidyasagar[7], the elements of the matrix C are obtained as

$$C_{kj} = \frac{1}{2}\sum_{i=1}^{n}\left[\frac{\partial D_{kj}}{\partial q_i} + \frac{\partial D_{ki}}{\partial q_j} - \frac{\partial D_{ij}}{\partial q_k}\right]\dot{q}_i \tag{33}$$

τ_f represents the joint torque vector due to friction. As pointed out by Craig[8], the total friction at each joint can be regarded as the sum of Coulomb friction and viscous friction. Coulomb friction is constant except for a sign dependence on the joint velocity. Viscous friction, in general, depends on various powers of joint velocity. However, higher powers contribute significantly only at high joint velocities. Manipulators usually do not attain such high velocities. Therefore, it is sufficient to consider only the linear dependence of viscous friction on joint velocity. Figure 2 shows a friction model consisting of Coulomb friction and linear viscous friction. Using this model, the joint friction torque vector can be represented as

$$\tau_f = X\,\mathrm{sgn}\{\dot{q}\} + \Gamma\dot{q} \tag{34}$$

where X is a diagonal matrix consisting of Coulomb friction constants for the joints, and Γ is a diagonal matrix consisting of viscous friction coefficients for the manipulator joints. The vector $\mathrm{sgn}\{\dot{q}\}$ is defined in a component-wise sense. It turns out that in many manipulator joints, friction also displays a dependence on joint position. However, such effects are not considered here. There are other effects like bending effects that are difficult to model and also neglected in the present model.

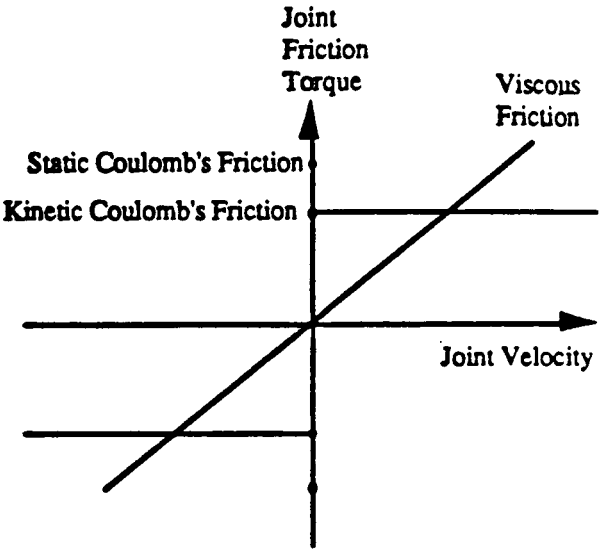

Fig. 2. Joint Friction Model Consisting of Coulomb's Friction and Linear Viscous Friction.

2.4 Base Motion

The translational velocity of the base center of mass can be written in terms of joint velocities by using the expression for Ω_B from Equation (19) in Equation (18).

$$V_B = -H_v^{-1}\left[H_{vq} - H_{v\Omega}M^{-1}Z\right]\dot{q} \tag{35}$$

Also, the base angular velocity from Equation (19) is

$$\Omega_B = -M^{-1}Z\dot{q} \tag{36}$$

Using the above expressions, the evolution of the base position and orientation with time can be determined.

3. Control System Design

Assuming that the dynamics of the space manipulator is described by Equation (31), where D and h are completely known, the feedback linearization or inverse dynamics[7] technique can be used to design controllers for tracking prescribed command trajectories for the joint angles. This can be accomplished as outlined in the following sub-section.

3.1 Feedback Linearization

Let the joint torque vector be of the following form.

$$\tau = Du + h \tag{37}$$

where u is the pseudo-control, i.e., it is the control input to the resulting linearized system. With the control law given by Equation (37), the closed-loop system becomes

$$\begin{bmatrix} \dot{q} \\ \ddot{q} \end{bmatrix} = A \begin{bmatrix} q \\ \dot{q} \end{bmatrix} + Bu \tag{38}$$

where

$$A = \begin{bmatrix} 0 & I \\ 0 & 0 \end{bmatrix}, B = \begin{bmatrix} 0 \\ I \end{bmatrix} \tag{39}$$

A simple PD (Proportional-Derivative) type of control law is chosen for the feedback linearized system

$$u = \ddot{q}_d + K_2(\dot{q}_d - \dot{q}) + K_1(q_d - q) \tag{40}$$

where K_1 and K_2 are proportional and derivative gain matrices, respectively. These matrices are usually chosen to be diagonal in order to achieve decoupled response among the joint angles. Substituting for u from Equation (40) into Equation (38), one obtains

$$\dot{e} = A_c e \tag{41}$$

where $e = \left[e_1^T \; e_2^T\right]^T$, $e_1 = q_d - q$, $e_2 = \dot{q}_d - \dot{q}$, $A_c = A - BK$, and $K = [K_1 \;\; K_2]$. If $K_1 > 0$ and $K_2 > 0$, the error dynamics as given by Equation (41) is asymptotically stable. The freedom in selecting the gain matrices can be utilized to meet performance specifications for the closed-loop system.

The preceding discussion assumes availability of perfect knowledge about the nonlinear system dynamics. However, in practice, D and h are usually imprecisely known due to modeling inaccuracies. For instance, the controller would be designed using the best estimates for friction coefficients. The actual joint friction might be different from that which is assumed for the controller design. Thus the controller uses computed versions of D and h. The objective here is to design a control law that is robust for bounded variations in D and h due to bounded uncertain dynamic effects. This issue of robust control design is discussed in the following sub-section, where it will be seen that the control law results in closed-loop asymptotic tracking.

3.2 Robust Feedback Linearization Using Passivity

In the presence of modeling uncertainties, let the control law be given as

$$\tau = \hat{D}u + \hat{h} + w \tag{42}$$

where $\hat{D}$ and $\hat{h}$ are computed versions of D and h, respectively. The additional feedback w(t) has been introduced to compensate for the modeling uncertainties. Substituting for τ and u from Equations (42) and (40) into Equation (31) it can be shown that the closed-loop system dynamics is given by

$$\dot{e} = A_c e + Bv \tag{43}$$

where

$$v = \Delta u + \delta \tag{44}$$

and

$$\Delta = \left[I - D^{-1}\hat{D}\right], \; \delta = D^{-1}\left[h - \hat{h} - w\right] \tag{45}$$

The first step in the proposed design is to choose the gain matrix $K = [K_1 \;\; K_2]$ and an output matrix F such that the linear system given by

$$\begin{aligned} \dot{e} &= A_c e + Bv \\ y &= Fe \end{aligned} \tag{46}$$

is SPR (Strictly Positive Real). This can be achieved as outlined in the following Theorem. A definition of the concept of Strictly Positive Realness can be found in Slotine and Li[9].

Theorem 1 [10]. Let K_1 and K_2 be such that

$$\begin{aligned} K_1 &= \text{diag}[k_{1i}];\; k_{1i} > 0,\; i = 1,\ldots,n \\ K_2 &= \text{diag}[k_{2i}];\; k_{2i} > 0,\; i = 1,\ldots,n \\ (k_{2i})^2 &> k_{1i}, \qquad i = 1,\ldots,n \end{aligned} \tag{47}$$

then if F = K, the system described by Equation (46) is SPR.

Note that the conditions of the Theorem as prescribed by (47) are extremely easy to satisfy.

With the linear System (46) being SPR, the Passivity Theorem[11] can be used to design asymptotically stable controllers as shown in the

following Theorem. The notation $\|x\|_T = \left(\int_0^T x^T x\,dt\right)^{1/2}$ is used in the sequel.

Theorem 2. Suppose that

(a) The desired trajectory for joint variables is such that $\ddot{q}_d \in L^2$.

(b) Finite β_1 and β_2 exist such that the uncertainty in h is bounded as follows.

$$\|h - \hat{h}\|_T \le \beta_1 \|u\|_T + \beta_2 \quad (\beta_1 \ge 0,\ \beta_2 \ge 0) \forall T \ge 0 \tag{48}$$

(c) The additional feedback w(t) in the control law of Equation (42) is of the following form.

$$w(t) = \alpha u(t) \quad (\alpha \ge 0) \tag{49}$$

Under these conditions, if α is chosen such that

$$\alpha > \lambda\left(\frac{\sigma_2 + \beta_1}{\sigma_1}\right) \tag{50}$$

where

$\sigma_1 \equiv \sigma_{min}(D)$, $\sigma_2 \equiv \sigma_{max}\left(D - \hat{D}\right)$, $\lambda \equiv \lambda_{max}(D)$; then the closed-loop System (43) is asymptotically stable.

Proof. The closed-loop system as given by Equation (43) can be represented in block diagram form as shown in Figure 3. It is first shown that the nonlinear block in the feedback path is passive[11].

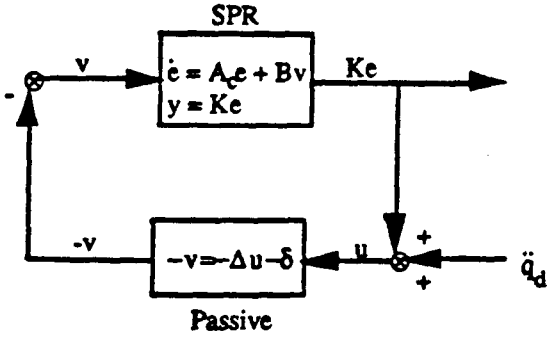

Fig. 3. Robust Feedback Linearization Using Passivity Theorem.

Consider

$$I = -\int_0^T u^T v\,dt \quad (T \ge 0) \tag{51}$$

From Equation (44), v is given as follows.

$$\begin{aligned} v &= \Delta u + \delta \\ &= \left[I - D^{-1}\hat{D}\right]u + D^{-1}\left[h - \hat{h} - w\right] \\ &= D^{-1}x - D^{-1}w \end{aligned} \tag{52}$$

where $x \equiv \left[D - \hat{D}\right]u + h - \hat{h}$. Substituting for v from Equation (52) into Equation (51), the integral becomes

$$I = \left(-\int_0^T u^T D^{-1} x\,dt\right) + \left(\int_0^T u^T D^{-1} w\,dt\right) \tag{53}$$

Let the first and second integrals on the right hand side be denoted by I_1 and I_2 respectively. Then

$$\begin{aligned} -I_1 &= \int_0^T u^T D^{-1} x\,dt \\ &\le \|u\|_T \|D^{-1}x\|_T \quad \text{(Hölder's Inequality)} \end{aligned} \tag{54}$$

Note that

$$\begin{aligned} \|D^{-1}x\|_T^2 &= \int_0^T x^T D^{-T} D^{-1} x\,dt \\ &\le \lambda_{max}\left(D^{-T}D^{-1}\right)\int_0^T x^T x\,dt \end{aligned} \tag{55}$$

and

$$\lambda_{max}\left(D^{-T}D^{-1}\right) = \sigma_{max}^2\left(D^{-1}\right) = \frac{1}{\sigma_{min}^2(D)} \equiv \frac{1}{\sigma_1^2} \tag{56}$$

Substituting for $\lambda_{max}\left(D^{-T}D^{-1}\right)$ from (56) into Inequality (55) and then taking the square root of both sides, one gets

$$\|D^{-1}x\|_T \le \frac{1}{\sigma_1}\|x\|_T \tag{57}$$

Using Inequality (57) in (54),

$$-I_1 \le \frac{1}{\sigma_1}\|u\|_T \|x\|_T \tag{58}$$

Recalling that $x = \left[D - \hat{D}\right]u + h - \hat{h}$, and using Schwarz's Inequality,

$$\|x\|_T \le \left\|\left[D - \hat{D}\right]u\right\|_T + \|h - \hat{h}\|_T \tag{59}$$

Since

$$\left\|\left[D-\hat{D}\right]u\right\|_T \le \sigma_{max}\left(D-\hat{D}\right)\|u\|_T = \sigma_2\|u\|_T, \qquad (60)$$

then Inequality (59) can be expressed using Inequalities (48) and (60) as

$$\|x\|_T \le (\sigma_2+\beta_1)\|u\|_T + \beta_2 \qquad (61)$$

Finally, using Inequality (61) in Inequality (58), a lower bound for I_1 is obtained in the following form.

$$I_1 \ge -\frac{1}{\sigma_1}\left[(\sigma_2+\beta_1)\|u\|_T^2 + \beta_2\|u\|_T\right] \qquad (62)$$

Now consider

$$\begin{aligned} I_2 &= \int_0^T u^T D^{-1} w\, dt \\ &= \alpha\int_0^T u^T D^{-1} u\, dt \\ &\ge \alpha\lambda_{min}\left(D^{-1}\right)\int_0^T u^T u\, dt \end{aligned} \qquad (63)$$

Noting that

$$\lambda_{min}\left(D^{-1}\right) = \frac{1}{\lambda_{max}(D)} \equiv \frac{1}{\lambda}, \qquad (64)$$

an upper bound for I_2 is obtained as follows.

$$I_2 \ge \frac{\alpha}{\lambda}\|u\|_T^2 \qquad (65)$$

Thus, using Inequalities (62) and (65) in Equation (53),

$$I \ge \left(\frac{\alpha}{\lambda} - \frac{\sigma_2+\beta_1}{\sigma_1}\right)\|u\|_T^2 - \frac{\beta_2}{\sigma_1}\|u\|_T \equiv f\left(\|u\|_T\right) \qquad (66)$$

It can be shown that if $\left(\frac{\alpha}{\lambda} - \frac{\sigma_2+\beta_1}{\sigma_1}\right) > 0$, then

$$f\left(\|u\|_T\right) \ge -\frac{(\beta_2/\sigma_1)^2}{4\left(\frac{\alpha}{\lambda} - \frac{\sigma_2+\beta_1}{\sigma_1}\right)} \qquad (67)$$

which in turn would imply

$$-\int_0^T u^T v\, dt \ge -\frac{(\beta_2/\sigma_1)^2}{4\left(\frac{\alpha}{\lambda} - \frac{\sigma_2+\beta_2}{\sigma_1}\right)} \quad \forall T \ge 0 \qquad (68)$$

Thus a sufficient condition for the nonlinear block to be passive is that $\alpha > \lambda\left(\frac{\sigma_2+\beta_1}{\sigma_1}\right)$.

Additionally, it is observed that the transfer function of the feedforward block $[A_c, B, K]$ is proper and has no poles on the imaginary axis. Hence it has finite gain[12]. Since according to Assumption (a) of the Theorem $\tilde{q}_d \in L^2$, then using the Passivity Theorem[11], one can conclude that the signals u, Ke, and v are bounded. Moreover, since the feedforward block is SPR, $Ke(t) = K_1 e_1(t) + K_2 e_2(t)$ goes to zero asymptotically. This in turn implies that $e_1(t)$ and $e_2(t)$ individually approach zero asymptotically[8].

Remarks.

(i) Some of the methods proposed in the past for designing robust controllers for robotics problems result in introduction of chattering in the control[7]. When the design method is modified to make the control smooth, closed-loop asymptotic tracking is generally compromised to some extent. In the control design proposed by Theorem 2, the achievement of robustness can be qualitatively understood as follows. The control law given by Equation (42) compensates for the uncertainty due to unknown D and h by employing additional feedback w. If the choice of w satisfies the assumptions of the Theorem, asymptotic stability for the joint error states is achieved.

(ii) The results of the Theorem are applicable to space manipulators as well as fixed base manipulators. Finally, it should be noted that the control design suggested using the results of the Theorem is not unique. First of all, w(t) need not be restricted to be of the form given by Equation (49) and second, even within the scope of the suggested design, there is a considerable amount of margin for performance optimization.

4. Simulation Results

The results of applying Theorems 1 and 2 in order to achieve a robust control design are illustrated for a planar single link space manipulator. Figure 4 shows such a planar one link space robot. A nonlinear dynamic model for the robot is obtained using the results of Section 2. Equation (31) describes the dynamics of this one degree of freedom system. The

system inertia, computed using Equation (28), turns out to be

$$D(q_1) = W_{1,1} - Z_{3,1}^2 / M_{3,3} \tag{69}$$

where

$$W_{1,1} = m_{01}p_1^2 + I_1 \tag{70}$$

$$Z_{3,1} = m_{01}p_1(p_0c_1 + p_1) + I_1 \tag{71}$$

$$M_{3,3} = m_{01}(p_0^2 + p_1^2 + 2p_0p_1c_1) + I_0 + I_1 \tag{72}$$

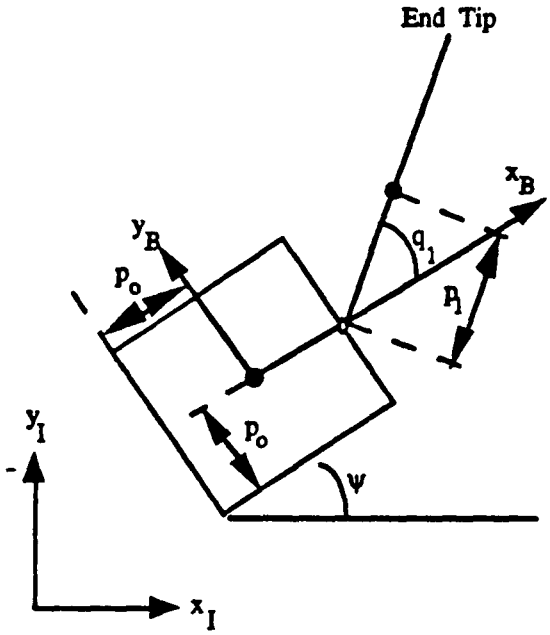

Fig. 4. A Single Link Planar Space Robot.

Using Equations (32) through (34), h is found to be

$$h(q_1, \dot{q}_1) = \frac{m_{01}p_0p_1s_1}{M_{3,3}^2}\left[m_{01}p_0(p_0 + p_1c_1) + I_0\right] \cdot \left[m_{01}p_1(p_0c_1 + p_1) + I_1\right]\dot{q}_1^2 + \chi sgn(\dot{q}_1) + \gamma\dot{q}_1 \tag{73}$$

where χ and γ are respectively the coefficients of Coulomb and viscous friction. In Equations (70) through (73) $m_{01} = m_0m_1 / m_e$, $m_e = m_0 + m_1$, $c_1 = \cos(q_1)$, and $s_1 = \sin(q_1)$.

- It can be seen easily that as $m_0 \to \infty$ and $I_0 \to \infty$,

$$D \to m_1p_1^2 + I_1, \quad h \to \chi sgn(\dot{q}_1) + \gamma\dot{q}_1 \tag{74}$$

which represents the case of a fixed base manipulator. Equation (35) is used to determine the evolution of the base position with time

$$\dot{x}_b = \frac{m_1}{m_e}\left[p_1s_{\psi 1} - \frac{Z_{3,1}}{M_{3,3}}\left(p_0s_\psi + p_1s_{\psi 1}\right)\right]\dot{q}_1$$

$$\dot{y}_b = \frac{m_1}{m_e}\left[-p_1c_{\psi 1} + \frac{Z_{3,1}}{M_{3,3}}\left(p_0c_\psi + p_1c_{\psi 1}\right)\right]\dot{q}_1 \tag{75}$$

where $s_{\psi 1} = \sin(\psi + q_1)$, $c_{\psi 1} = \cos(\psi + q_1)$. Finally, the base attitude dynamics is obtained using Equation (36):

$$\dot{\psi} = -\frac{Z_{3,1}}{M_{3,3}}\dot{q}_1 \tag{76}$$

Assuming that no modeling uncertainty exists, a feedback linearizing controller is designed for the one link space manipulator using the control law given by Equation (37). Simulation is carried out using automatic step size second and third order Runge-Kutta-Fehlberg integration methods[13]. Table I lists physical parameters of the example robot used in the simulation. Note that the base and link masses are assumed to be of the same order of magnitude. The values of Coulomb and viscous friction coefficients are taken to be

$$\chi = 0.5 \text{ N-m}, \quad \gamma = 2.0 \text{ N-m-s/rad} \tag{77}$$

Closed-loop results are generated for a step command of 1 radian to the joint angle. The feedback gains are chosen to be $k_1 = 0.4$ and $k_2 = 1.0$. This choice of gains satisfies Conditions (47) and yields a closed-loop response without any overshoot, as shown in Figure 5.

Table I. Physical Parameters of Single Link Planar Space Robot.

Body	p (meter)	l (meter)	m (kg)	I (kg.m^2)
0 (Base)	3.0	-	5.0	30.0
1 (Link)	3.0	6.0	1.0	3.0

Next, it is assumed that the value of the Coulomb friction coefficient, χ is unknown, but that

$$0.5 \le \chi \le 0.75 \tag{78}$$

Since uncertainty exists in the h vector, the computed version of h is given by

$$\hat{h} = h|_{\chi \to \hat{\chi}} \tag{79}$$

where $\hat{\chi} = 0.5$, which is the nominal value of the Coulomb friction coefficient. The response of the controller with $\chi = 0.75$ and without any additional

feedback is shown in Figure 6. It can be seen that there is a steady-state error in the joint angle response. The steady-state error in this particular instance can be eliminated by adding an integral feedback term to the control law given by Equation (40); however, this is accompanied by a large overshoot. Hence, a need exists for making the control law robust with respect to the uncertainty. The results of Theorem 2 are used for the design. It is first noted that

$$\left\|h-\hat{h}\right\|_T = \left\|(\chi-\hat{\chi})\mathrm{sgn}(\dot{q}_1)\right\|_T = \left|\chi-\hat{\chi}\right|\left[\int_0^T [\mathrm{sgn}(\dot{q}_1)]^2\,dt\right]^{1/2} \qquad (80)$$

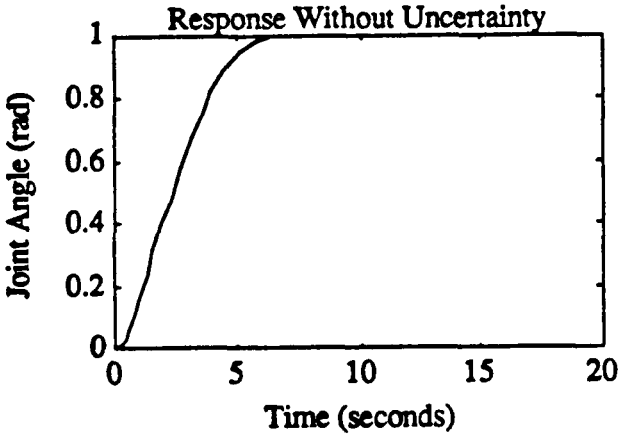

Fig. 5. Joint Angle Response With No Modeling Uncertainty.

Clearly, $\left\|h-\hat{h}\right\|_T$ is maximum when $|\chi-\hat{\chi}|$ is maximum. Hence the controller is designed for χ = 0.75, and it works for all other values of χ lying in the range indicated by (78). The design involves determining a suitable value of α that satisfies Inequality (50), assuming that finite β_1 and β_2 exist for the bound given by Inequality (48). Figure 7 shows the variation of system inertia, D, given by Equation (69), with respect to the joint angle. From this plot, it is easily found that λ = 10.2273, and σ_1 = 5.3571. Clearly, by definition, σ_2 = 0. Hence the requirement (50) of Theorem 2 translates to:

$$\alpha > 1.91(\beta_1) \qquad (81)$$

The values of β_1 and β_2 are obtained in an iterative manner. Starting with an assumed set of values for these parameters, closed-loop simulation is performed with the resulting value of α as obtained by Condition (81). If the joint error states are not asymptotically stable, this implies that Inequality (48) must have been violated. The amount by which violation occurs is used as a measure to update the estimates of β_1 and β_2. The process is repeated until convergence is obtained. For the present example, it was found that β_1 = 12.5 and β_2 = 1.5 satisfy Inequality (48). This resulted in a choice of α = 25.0 for the design. Note that the process implicitly assumes at the outset that condition (b) of Theorem 2 will hold.

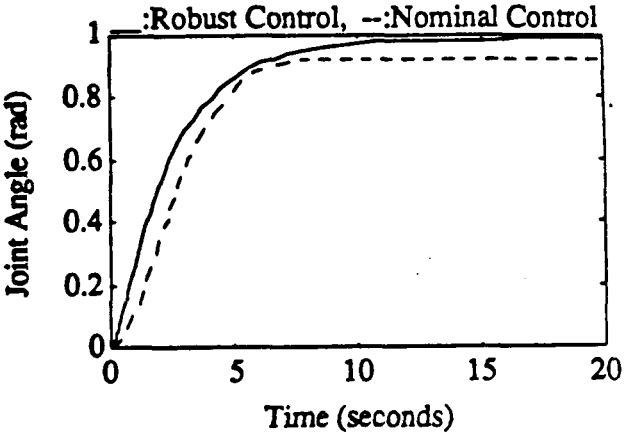

Fig. 6. Joint Angle Response With Bounded Uncertainty in Friction Modeling.

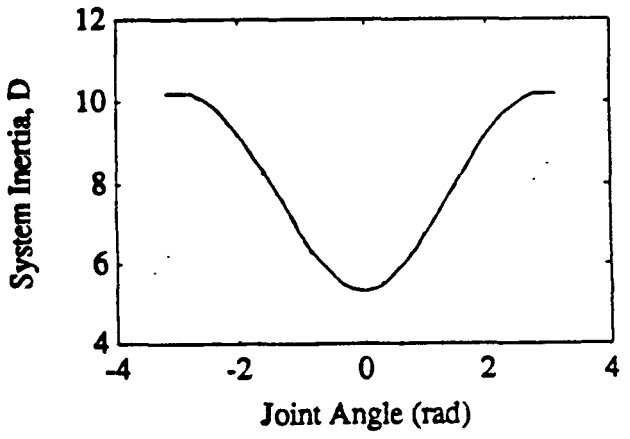

Fig. 7. Variation of System Inertia Matrix With the Joint Angle.

Figures 6 and Figures 8 through 12 show the closed-loop responses for the design, with and without the inclusion of additional feedback. Figure 6 shows that asymptotic tracking in the joint angle is achieved in the face of uncertainty. Figures 9 and 10 show that the base moves in reaction to link motion; this is due to the conservation of linear and angular momenta as discussed in Section 2. Figure 11 depicts the

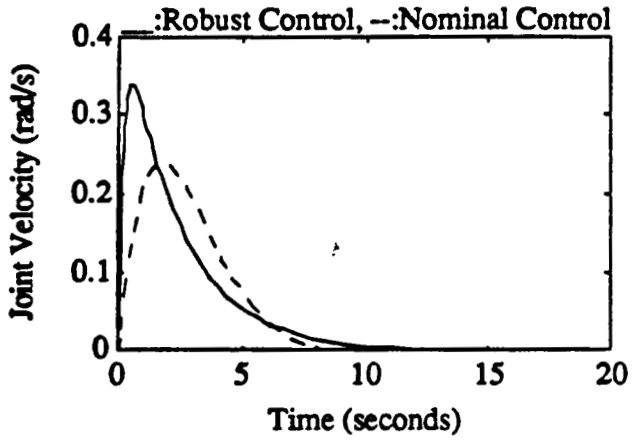

Fig. 8. Joint Velocity Response With Bounded Uncertainty in Friction Modeling.

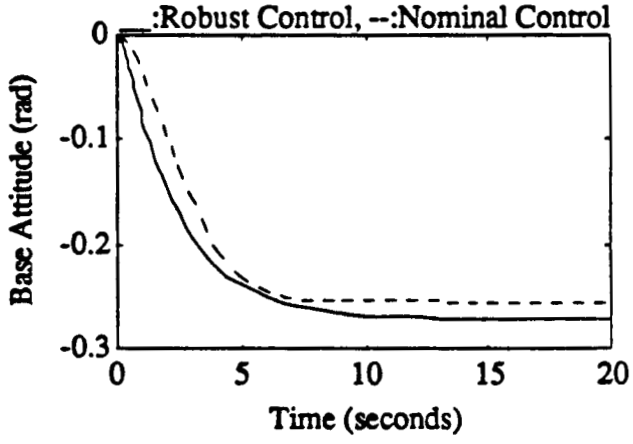

Fig. 9. Base Attitude Response With Bounded Uncertainty in Friction Modeling.

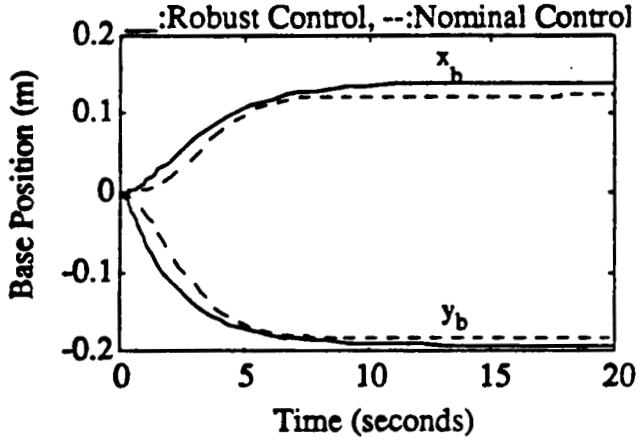

Fig. 10. Base Position Response With Bounded Uncertainty in Friction Modeling.

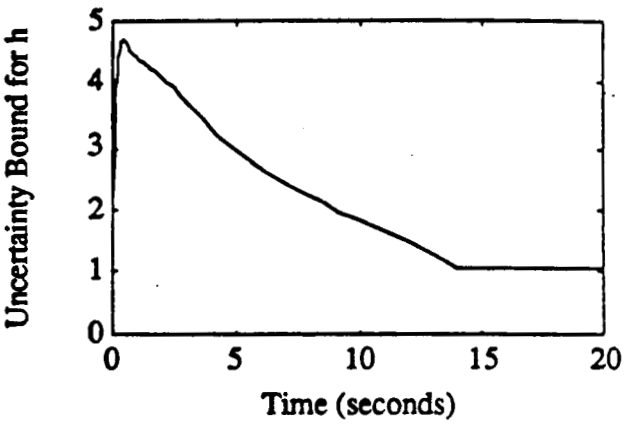

Fig. 11. The Quantity $\beta_1\|u\|_T + \beta_2 - \|h - \hat{h}\|_T$ With Bounded Uncertainty in Friction Modeling.

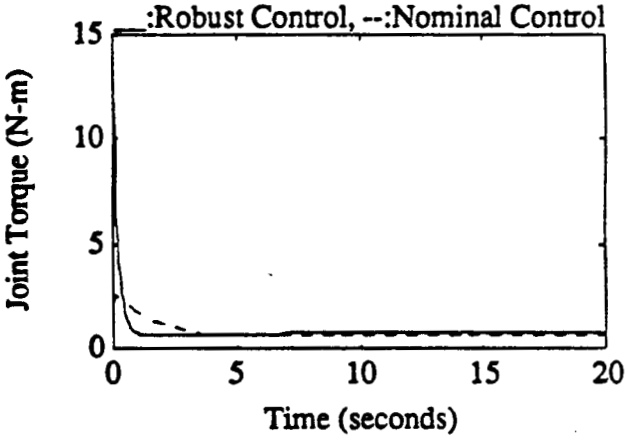

Fig. 12. Joint Torque Input With Bounded Uncertainty in Friction Modeling.

satisfaction of Inequality (48). Figure 12 shows the joint torque input requirements. It was confirmed through simulations that the controller designed works well for any value of χ within the range indicated by (78). Indeed for any value of $\chi < 0.75$, the uncertainty bound on h is satisfied by a greater margin.

5. Conclusions

A nonlinear dynamic model was obtained for space manipulators with uncontrolled base. A robust control method based on feedback linearization and passivity concepts was proposed for space manipulators. The method is applicable to fixed base manipulators as well. The control law results in asymptotic joint angle tracking in the face of bounded uncertainties such as those due to imprecise friction modeling.

References

[1]. E. Papadopoulos and S. Dubowsky, "On the Nature of Control Algorithms for Space Manipulators," Proceedings of the IEEE International Conference on Robotics and Automation, Cincinnati, Ohio, May 1990, pp. 1102-1108.

[2]. Z. Vafa and S. Dubowsky, "The Kinematics and Dynamics of Space Manipulators: The Virtual Manipulator Approach," *The International Journal of Robotics Research*, Vol. 9, No. 4, August 1990, pp. 3-21.

[3]. H. L. Alexander and R.H. Cannon, "Experiments on the Control of a Satellite Manipulator," Proceedings of the American Control Conference, Minneapolis, Minnesota, June 1987.

[4]. K. Yoshida and Y. Umetani, "Control of Space Manipulators with Generalized Jacobian Matrix," in *Space Robotics: Dynamics and Control*, Eds. Y. Xu and T. Kanade, Kluwer Academic Publishers, Boston, Massachusetts, 1993, pp. 165-204.

[5]. C. -H. Chuang, M. Mittal, and J. -N. Juang, "Passivity Based Robust Control of Space Manipulators," Proceedings of the AIAA Guidance, Navigation, and Control Conference, Monterrey, California, August 1993.

[6]. Y. Masutani, F. Miyazaki, and S. Arimoto, "Sensory Feedback Control For Space Manipulators," Proceedings of the 1989 IEEE International Conference on Robotics and Automation, Scottsdale, Arizona, May 1989, pp. 1346-1351.

[7]. M. W. Spong and M. Vidyasagar, *Robot Dynamics and Control*, John Wiley, New York, 1989.

[8]. J. J. Craig, *Introduction to Robotics Mechanics and Control*, Second Edition, Addison-Wesley, 1989, pp. 214-215.

[9]. J-J. E. Slotine and W. Li, *Applied Nonlinear Control*, Prentice Hall, New Jersey, 1991, pp. 127, 399.

[10]. C. Abdallah and R. Jordan, "A Positive-Real Design for Robotic Manipulators," Proceedings of the 1990 American Control Conference, San Diego, California, May 1990, pp. 991-992.

[11]. C. A. Desoer and M. Vidyasagar, *Feedback Systems: Input-Output Properties*, Academic Press, New York, 1975, pp. 173-186.

[12]. J. C. Doyle, B. A. Francis, and A. R. Tannenbaum, *Feedback Control Theory*, Macmillan, New York, 1992, pp. 16.

[13]. MATLAB Reference Guide, The MathWorks Inc., August 1992, pp. 351-353.